

A consistent regional dataset of dissolved oxygen in the Western Mediterranean Sea (2004-2023): CTD-O2WMED

Malek Belgacem¹, Katrin Schroeder¹, Marta Álvarez², Siv K. Lauvset³, Jacopo Chiggiato¹, Mireno Borghini⁴, Carolina Cantoni⁵, Tiziana Ciuffardi⁶, Stefania Sparnocchia⁵

¹ CNR-ISMAR, Arsenale Tesa 104, Castello 2737/F, 30122 Venice, Italy

² Instituto Español de Oceanografía, IEO-CSIC, A Coruña, Spain

³ NORCE Norwegian Research Centre, Bjerknes Centre for Climate Research, Bergen, Norway

⁴ CNR-ISMAR, Via Santa Teresa, Pozzuolo di Lerici, 19032 La Spezia, Italy

⁵ CNR-ISMAR, Area Science Park, Basovizza, 34149 Trieste, Italy

⁶ Department of Sustainability, St Teresa Marine Environment Research Centre, ENEA, Pozzuolo di Lerici, 19032 La Spezia, Italy

Correspondence to: Malek Belgacem (malek.belgacem@ve.ismar.cnr.it)

Formatted: Italian (Italy)

Field Code Changed

Abstract. A new dataset from oceanographic cruises in the Western Mediterranean Sea (WMED) was compiled to integrate the previously published regional data product CNR-DIN-WMED about dissolved inorganic nutrients (Belgacem et al., 2019, 2020). The Mediterranean region is experiencing rapid changes, necessitating high-quality and reliable datasets. However, the scarcity of the in-situ observations hinders the understanding of these changes and their impact on biogeochemical cycles. Dissolved oxygen is a vital component of marine ecosystems and plays a fundamental role in governing nutrient and carbon cycles, underscoring the need for accurate and reliable data. To address this, a high-resolution, regional-scale data product was developed to understand decadal variability and spatial/temporal patterns of the ventilation process in the WMED. This study presents an extensive collection of unpublished dissolved oxygen data from continuous sensors collected between 2004 and 2023, along with a description of the quality control procedures. The quality assurance process involves calibration of CTD measurements against Winkler analyses and the comparison of deep observations with reference datasets, using the crossover analysis. The resulting data product O2WMED can be used as reference for assessing oxygen sensors mounted on biogeochemical-Argo (BGC-Argo) floats or Gliders and for regional model validation.

The Mediterranean Sea is undergoing rapid change, highlighting the urgent need for high-quality, long-term datasets to investigate changes and assess impacts on its complex biogeochemical cycles. While dissolved inorganic nutrients have been well documented in the Western Mediterranean Sea (WMED) through DIN-WMED data product (Belgacem et al., 2019, 2020), reliable oxygen data have remained scarce, despite dissolved oxygen being a key driver of marine ecosystem health and central to carbon and nutrient cycling.

To fill this gap, we compiled and rigorously quality-controlled a new regional-scale dataset: CTD-O2WMED. This product comprises over 1000 unpublished high-resolution vertical profiles of sensor-based dissolved oxygen measurement collected between 2004 and 2023. The quality check process includes sensor post calibration assessment, primary quality check and a secondary quality check based on crossover analysis with established deep reference datasets, ensuring consistency and accuracy across space and time.

CTD-O2WMED provides an essential observational basis for assessing decadal oxygen variability, tracking anomalies, and improving our understanding of ventilation processes in the WMED. It also serves as a benchmark

for calibrating oxygen sensor on BGC-Argo floats, and for validating regional biogeochemical models. This dataset represents a critical step toward more accurate estimation of oxygen trends in the Mediterranean Sea, an increasingly vital metric in the context of global deoxygenation and climate change.

Formatted: English (United States)

Data coverage

Coverage: 44° N–35° S, 6° W–14° E
Location name: western Mediterranean Sea
Date/time start: October 2004
Date/time end: April 2023

1 Introduction

Oxygen plays a crucial role as a fundamental oceanic variable. The ocean produces about 50% of the earth's oxygen, which is crucial for the atmospheric oxygen inventory (Grégoire et al., 2023). The ocean's oxygen levels are highly susceptible to changes in the last decades.

leading to high surface productivity and cause the sinking of organic matter which stimulate oxygen consumption in the deep sea, leading to the creation of the Oxygen Minimum zones (OMZs). The OMZs can become larger, more intense in coming decades and low oxygen events can become more frequent.

Formatted: English (United States)

As we face warming ocean and increased stratification, the anticipated decline in oxygen levels may lead to enhanced acidification and reduced CaCO_3 , potentially accelerating in the remineralization of organic matters at shallower depths. Consequently, the expansion of low oxygen zones is expected, posing significant ecological challenges (Keeling and al., 2009).

Increased degradation of organic matter in the deep ocean intensifies dissolved oxygen consumption. Warming conditions contribute to the heightened stratification periods and an intensification of the pycnocline, impacting biological activity and thus dissolved oxygen consumption. Additionally, factors such as denitrification and the extension of the OMZs can influence the nitrogen: phosphorus (N:P) ratio and the levels of primary productivity. Warming seawater, increased stratification and higher CO_2 levels have reshaped community distribution and ecosystem composition, resulting in decreased dissolved oxygen levels (Grégoire et al., 2023).

The decline in oxygen can be attributed to lower solubility rates due to warming and increased water column stratification, reducing the downward diffusion and mixing of well-oxygenated surface waters towards deeper layers. Such changes in oxygen concentration can trigger variations in the biological loop and the distribution of biogeochemical tracers, which have significant implications for marine ecosystems, particularly in vulnerable hotspots.

The Mediterranean Sea has been notably affected by these changes, especially in the past decade, characterized by frequent marine heat waves episodes (Marullo et al., 2023; Martinez et al., 2023; Pastor and Khodayar et al., 2023). Rising temperatures can disturb the distribution and availability of dissolved oxygen in seawater (Reale et al.,

2022; Alvaréz et al., 2023). The region's enclosed nature and its peculiar thermohaline circulation further complicates the understanding of oxygen dynamics (Powley et al., 2016). Subsequently, Observational efforts, such as the Medar/Medatlas project (Fichaut et al., 2003), the MED-SHIP transects (<https://www.go-ship.org/>) (Schroeder et al., 2015), have provided valuable insights, but uncertainties remain regarding the long-term impacts of deoxygenation and acidification on Mediterranean marine ecosystems (Coppola et al., 2018).

To address these pressing issues, a compilation of oxygen observations collected by the Italian National Research Council (CNR), between 2004 and 2023 in the Western Mediterranean Sea (WMED) is documented. This effort aims to provide reliable measurements of dissolved oxygen, thereby enhancing our understanding of biogeochemical cycling and ventilation in the region. The purpose of this paper is to describe the oxygen data collected by the CNR and report the quality control procedure to justify the recommended corrections applied to the oxygen profiles.

Oxygen in the ocean is primarily produced via photosynthesis in the surface layer by phytoplankton, especially in regions of high primary productivity. The export and remineralization of organic matter from the surface, lead to oxygen consumption at depth. This can give rise to oxygen minimum zones (OMZs) or Oxygen minimum layers (OMLs), where biological respiration exceeds oxygen supply. While OMZs are prominent in certain oceanic regions, the Mediterranean Sea is generally well-oxygenated and does not exhibit OMZ but rather OML. Nevertheless, localized low oxygen events may become more frequent and intense due to ongoing climate changes (Grégoire et al. 2023).

Ocean warming and increased stratification reduce oxygen solubility and inhibit vertical mixing, thereby limiting the downward transport of oxygen-rich surface waters. These processes contribute to the expansion and intensification of low-oxygen zones, with implications for biogeochemical cycling, ecosystem function, and carbon export (Keeling et al., 2009). In deep ocean, enhanced remineralization and reduced ventilation can further exacerbate oxygen loss. Moreover, denitrification under low-oxygen conditions can alter Nitrogen to Phosphorus (N:P) ratio, influencing primary productivity and nutrient cycling.

Increased CO₂ levels and stratification also reshape biological communities and potentially lowering ecosystem resilience. These biogeochemical shifts affect the distribution of Oxygen and other tracers, particularly in semi-enclosed basins such as the Mediterranean Sea.

The Mediterranean Sea has experienced significant changes in recent decades, including recurrent marine heatwaves (Marullo et al., 2023; Martinez et al., 2023; Pastor and Khodayar et al., 2023), which affect oxygen distribution (Reale et al., 2022; Alvarez et al., 2023). The region's semi-enclosed nature and complex thermohaline circulation and regional differences amplify its sensitivity to climate variability (Powley et al., 2016; Testor et al. 2017; Margirier et al., 2020).

Two major events have notably altered the Mediterranean thermohaline structure. In the eastern Mediterranean (EMED), the eastern Mediterranean transient (EMT) of the mid-1990s shifted deep water formation source from colder, less saline Adriatic Deep water to warmer, more saline Aegean/Cretan Water. This new deep-water mass ventilated the Levantine basin and the Ionian Sea around 1999 and reached the Sicily channel by 2001. When the Aegean water weakened, the Adriatic deep water became dominant again between 2000 and 2010, though in subsequent years it failed to reach the deepest Ionian layers, ventilating instead the 2000-3000 m range

Field Code Changed

In the Western Mediterranean Sea (WMED), deep convection in the Gulf of Lion, has traditionally maintained the ventilation of the Western Mediterranean Deep Water (WMDW). A peak in deep water renewal occurred during the Western Mediterranean Transient (WMT) around year 2004. Since then, a decline in both the frequency and intensity of deep convection has been observed (Fourrier et al., 2020 ;Li and Tanhua, 2020), leading to a weakening of ventilation and intensification of the oxygen minimum at intermediate depths and affecting the uptake of atmospheric oxygen (Ulses et al., 2021).

Long-term observational programs such as the Medar/Medatlas (Fichaut et al., 2003), MED-SHIP (Schroeder et al., 2015), and MOOSE (Coppola et al., 2018) have provided valuable insights of these changes. Recent studies are using Machine learning to reconstruct higher temporal and spatial resolution Oxygen datasets by satellite and other data sources (Liu et al., 2025). Yet, uncertainties remain about long-term impacts of deoxygenation and acidification on Mediterranean marine ecosystems (Coppola et al., 2018; Alvarez et al. 2014).

To improve understanding of regional dissolved oxygen dynamics and the impact on biogeochemical trends, this study presents a quality-controlled compilation of CTD oxygen profiles collected by the Italian National Research Council (CNR) between 2004 and 2023 in the WMED. The dataset offers reliable CTD oxygen data that can support assessments of water mass ventilation and long-term variability. This paper document the dataset and described the quality control procedures, including calibration assessments and corrections, to ensure the scientific reliability of oxygen measurements.

2 Dissolved oxygen data collection

2.1 The CNR data collection

The CTD-Oxygen in the WMED (CTD-O2WMED) dataset contains 1,382 CTD oxygen profiles collected within 25 cruises. In Figure 1, the spatial distribution of CTD profiles is depicted, highlighting the extensive coverage across the Northern Western Mediterranean (WMED) and key hydrographic transects.

Measures are concentrated in the eastern part of the WMED: the subregions of the Ligurian sea, Tyrrhenian and along the Tunisia-Sicily-Sardinia area. Spanning two decades from 2004 to 2023, the dataset exhibits robust temporal coverage, particularly between 2004 and 2015 (see Fig.2a). In particular, the years 2005, 2006, 2010, and 2012 stand out with the highest number of CTD stations, coinciding with years that included monthly surveys, indicating a more frequent repeat frequency (see Fig. 2). While reasonable temporal coverage is observed between 2004 and 2015 (except for 2014), the availability of stations diminishes between 2016 and 2023.

Formatted: Space After: 0 pt

143

144

145

146

147

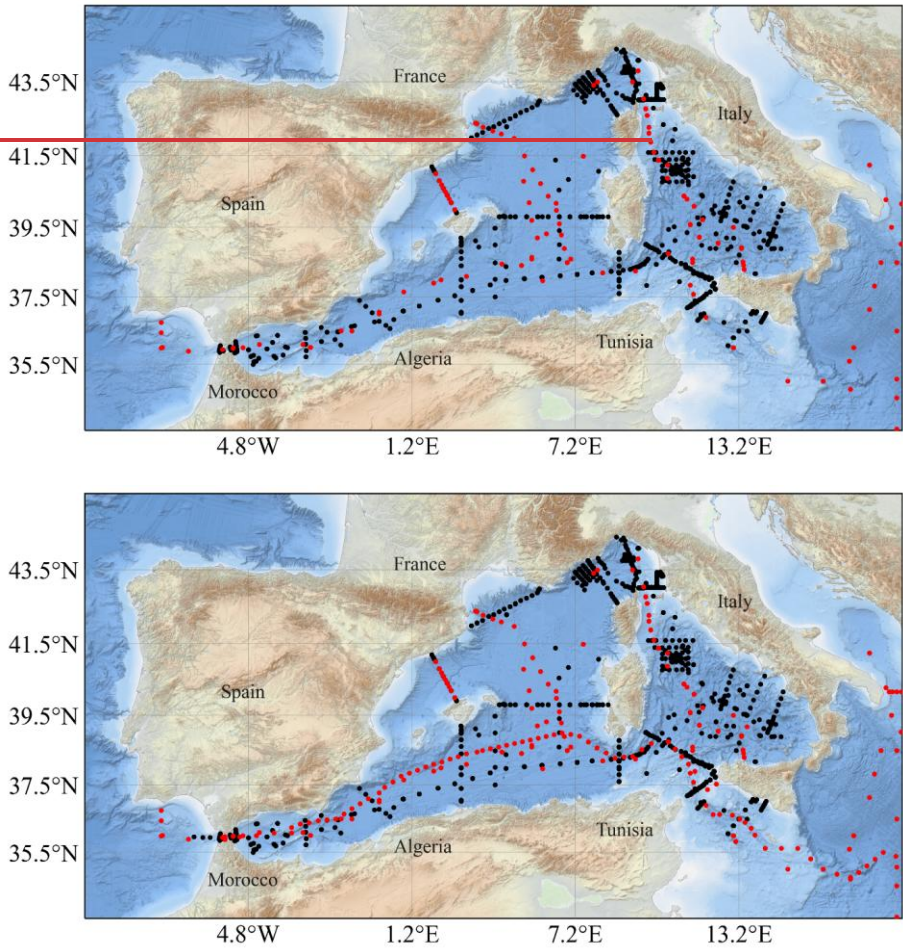
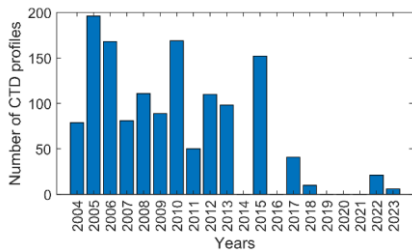
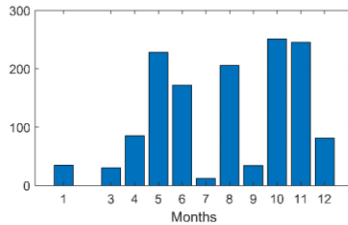


Figure 1. Spatial distribution of cruise stations with CTD oxygen data (black dots) in the **CTDO2_** WMEDv1 CNR dataset across the WMED. The red markers indicate stations from **selected-the** reference cruises.

(a)



(b)



Formatted: Font: (Default) +Body (Calibri), 11 pt, Not Bold, Complex Script Font: +Body CS (Arial), 11 pt, Not Bold, English (United States)

Figure 2. Temporal distribution of CTD profiles with oxygen in the O2WMED-CNR dataset: A. annual distribution and B. monthly distribution.

- Assessment of sensor calibration

Dissolved oxygen has been measured using Sea-Bird (SBE43) oxygen sensor mounted on the CTD rosette, and by Winkler titration of discrete samples collected in Niskin bottles at various depths. These samples were analyzed onboard by different research team. In this dataset, we only evaluate the CTD sensor oxygen data, which were post-calibrated against Winkler measurements as summarized in Figure 3. Note that discrete Winkler data are not included in the final product.

The cruises listed in Table 1 were calibrated using Winkler titrations, following standard procedures (Grasshoff et al. 1983; Langdon, 2010). Discrete samples were used to calibrate the CTD sensor, correcting for sensor drift, in line with the approaches of Janzen et al. (2007) and Uchida et al. (2010). Calibration methods followed the application note SBE 43 DO Sensor calibration and data correction (NO.64-2 from Sea-Bird Electronics, www.seabird.com).

Following Uchida et al. (2010), we assess the residuals between Winkler (O2 bottle) sensor (O2 sensor) after calibration, or calibration limitations. Sensor data were matched to discrete samples based on pressure. For cruises where more than one SBE43 sensor was deployed, the sensor with the smallest residuals relative to the Winkler samples was selected for this assessment.

Figure 3(a) shows of the residuals (O2 bottle–O2 sensor) plotted against pressure, with cruises color-coded by start date. residuals are generally smaller below 800 db, though systematic differences up to $\pm 15 \mu\text{mol/kg}$ are observed. Figure 3(b) presents the residual distribution for each cruise using boxplots. High variability (standard deviation of the mean residual $> 7 \mu\text{mol/kg}$) is observed for cruises such as 48UR20080905, 48UR20050412, 48QL20171023 and 48UR20041006.

In 48UR20080905, only five Winkler samples limiting calibration quality. For 48UR20050412, which had two legs samples from one leg were used to calibrate the entire cruise. Some cruises (e.g., 48UR20060608) show pressure-dependent residuals, indicating issues with pressure compensation during calibration.

Figure 3(c) summarized cruise-level agreement using the mean residual and the percentage of values within $\pm 2 \mu\text{mol/kg}$. According to Uchida et al., (2010), residuals should remain within this threshold after proper calibration. Cruises were color-coded as follows: Green indicates cruises where $\geq 40\%$ of residuals within $\pm 2 \mu\text{mol/kg}$ (considered good agreement); Blue represent moderate or uncertain agreement (19 to $<40\%$ of mean residual within $\pm 2 \mu\text{mol/kg}$); Grey denotes cruises with systematic bias ($<19\%$ of mean residual $> 2 \mu\text{mol/kg}$).

Eight cruises show good agreement, eleven are moderate, and the rest display systematic positive or negative biases. These may reflect sensor calibration issues, bottle handling problems, or sensor drift. This analysis helps flag suspect data for correction or further review. We do not discuss each cruise individually, as the purpose here is to assess the outcome of the calibration process.

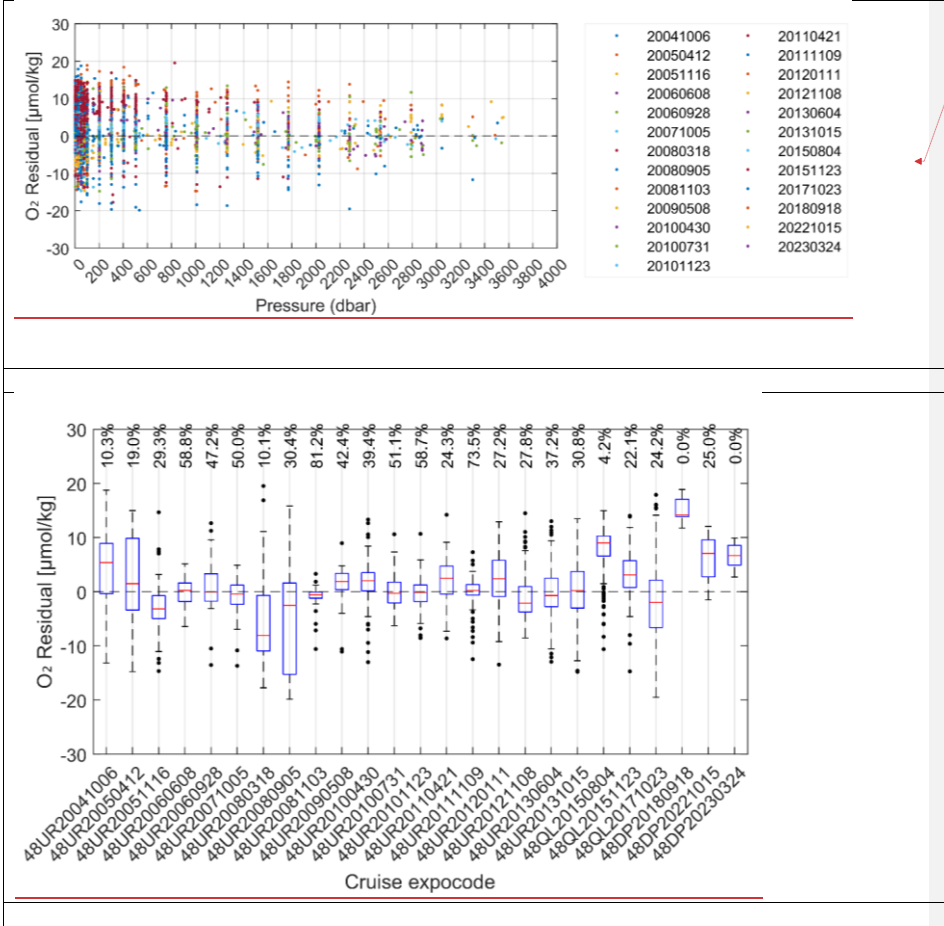
attached

Data included in the dataset (Table 1) were routinely calibrated against Winkler measurements following Grasshoff et al. (1983) and Langdon (2010). Discrete samples were used to calibrate the CTD sensor to correct any potential

185 bias and adjust drift in the SBE 43 oxygen sensor following Janzen et al. (2007) and Uchida et al. (2010). Details
186 regarding the post calibration against Winkler observation can be found in the supplementary materials (Table
187 S1).

Formatted: English (United States)

Formatted Table



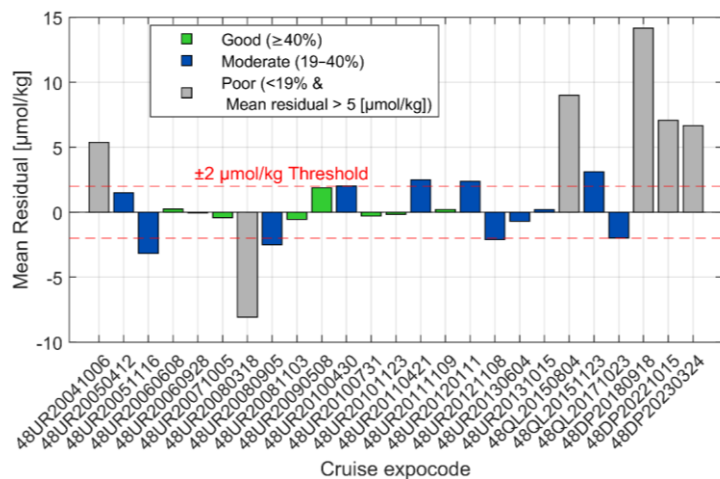


Figure 3. Residuals between CTD oxygen data from SBE43 (sensor) and Winkler oxygen data (O2 bottle) for (a) all dataset against pressure color coded with each cruise starting date; (b) boxplot distribution with % of residuals within $\pm 2 \mu\text{mol/kg}$ and, (c) assessment of the mean residual of each expocode/cruise.

Table 1. Cruise summary table listed with number of stations. Refer to Belgacem et al. (2020) and Ribotti et al. (2022) for cruise metadata.

Table 1. Cruise summary table listed with number of stations. Refer to Belgacem et al. (2020) and Ribotti et al. (2022) for cruise metadata.

Cruise ID no.	Common name	EXPCODE	Date Start/End	CTD profiles	Maximum bottom depth (m)
2	MEDGOOS9	48UR20041006	6 – 25 OCT 2004	79	3668
2	MEDOCC05/MFSTEP2	48UR20050412	24 APR – 16 MAY 2005	160	3657
2	MEDGOOS11	48UR20051116	16 NOV – 3 DEC 2005	36	3494
2	MEDOCC06	48UR20060608	8 JUN – 3 JUL 2006	127	2882
2	MEDGOOS13/MEDBIO06	48UR20060928	28 SEP – 8 NOV 2006	41	4137
2	MEDOCC07	48UR20071005	5 – 29 OCT 2007	81	3497

Commented [MB1]: Toste: Maybe add a column on which oxygen sensor was used, and if there was a post-calibration needed after comparison with Winkler data.

Formatted: English (United States)

Formatted Table

Formatted: English (United States)

Formatted: English (United States)

Formatted: English (United States)

Formatted: English (United States)

Formatted: English (United States)

Formatted: English (United States)

205

10	SESAMEIt4 KM3 or SESAME_KM3	48UR20080318	18 MAR - 7 APR 2008	27	3510
11	SESAMEIt5 (Sesame KM3 September 2008)	48UR20080905	5 - 16 SEP 2008	24	3450
12	MEDCO08	48UR20081103	3 - 24 NOV 2008	60	3443
13	TYRRMOUNTS	48UR20090508	8 MAY - 3 JUN 2009	89	3509
14	BIOFUN010	48UR20100430	30 APR - 17 MAY 2010	29	3541
15	VENUS1	48UR20100731	31 JUL - 25 AUG 2010	116	3649
16	BONISIC2010	48UR20101123	23 NOV - 9 DEC 2010	24	3539
17	EUROFLEET11	48UR20110421	21 APR - 8 MAY 2011	31	3541
18	BONIFACIO2011	48UR20111109	9 - 23 NOV 2011	18	3542
20	ICHNUSSA12	48UR20120111	11 - 27 JAN 2012	35	3552
21	EUROFLEET2012	48UR20121108	8 - 26 NOV 2012	75	3554
211	VENUS_2	48UR20130604	4 - 25 JUN 2013	59	3539
22	ICHNUSSA13	48UR20131015	15 - 29 OCT 2013	40	3542
222	ICHNUSSA15	48QL20151123	23 NOV - 14 DEC 2015	62	3633
23	OCEANCERTAIN15	48QL20150804	4 - 18 AUG 2015	90	3514
24	ICHNUSSA17/INFRAOCE17	48QL20171023	23 OCT - 28 NOV 2017	41	3537
25	ICHNUSSA/JERICO18	48DP20180918	18-25 SEP 2018	10	525
27	JERICO-II-2022	48DP20221015	15 - 25 OCT 2022	21	1004
28	JERICO-III-EurogoShip-2023	48DP20230324	24 MAR - 09 APR 2023	6	909

206

Cruise ID	Cruise	Expocode	Research vessel (RV)	Date Start/End	Nb CTD profile
2	MEDGOOS9	48UR20041006	Urania	6 - 25 OCT 2004	82
3	MEDOCC05/ MFSTEP2	48UR20050412	Urania	24 APR - 16 MAY 2005	160
5	MEDGOOS11	48UR20051116	Urania	16 NOV - 3 DEC 2005	36
6	MEDOCC06	48UR20060608	Urania	8 JUN - 3 JUL 2006	127
8	MEDGOOS13/MEDBIO06	48UR20060928	Urania	28 SEP - 8 NOV 2006	41
9	MEDOCC07	48UR20071005	Urania	5 - 29 OCT 2007	81
10	SESAMEIt4 KM3 or SESAME_KM3	48UR20080318	Urania	18 MAR - 7 APR 2008	27
11	SESAMEIt5 (Sesame KM3 September 2008)	48UR20080905	Urania	5 - 16 SEP 2008	24
12	MEDCO08	48UR20081103	Urania	3 - 24 NOV 2008	60
13	TYRRMOUNTS	48UR20090508	Urania	8 MAY - 3 JUN 2009	86
14	BIOFUN010	48UR20100430	Urania	30 APR - 17 MAY 2010	29
15	VENUS1	48UR20100731	Urania	31 JUL - 25 AUG 2010	116
16	BONISIC2010	48UR20101123	Urania	23 NOV - 9 DEC 2010	24
17	EUROFLEET11	48UR20110421	Urania	21 APR - 8 MAY 2011	31
18	BONIFACIO2011	48UR20111109	Urania	9 - 23 NOV 2011	18
20	ICHNUSSA12	48UR20120111	Urania	11 - 27 JAN 2012	35
21	EUROFLEET2012	48UR20121108	Urania	8 - 26 NOV 2012	75
211	VENUS_2	48UR20130604	Urania	4 - 25 JUN 2013	59
22	ICHNUSSA13	48UR20131015	Urania	15 - 29 OCT 2013	40
222	ICHNUSSA15	48QL20151123	Minerva Uno	23 NOV - 14 DEC 2015	62
23	OCEANCERTAIN15	48QL20150804	Minerva Uno	4 - 18 AUG 2015	90
24	ICHNUSSA17/INFRAOC E17	48QL20171023	Minerva Uno	23 OCT- 28 NOV 2017	41
25	ICHNUSSA/JERICO18	48DP20180918	DallaPorta	18-25 SEP 2018	10
27	JERICO-II-2022	48DP20221015	DallaPorta	15 - 25 OCT 2022	21
28	JERICO-III-EurogoShip- 2023	48DP20230324	DallaPorta	24 MAR - 09 APR 2023	6

206

207

208

209

210

The vertical distribution of dissolved oxygen in the WMED reflects the interplay between air-sea gas exchange, biological activity, and regional circulation processes. In the surface waters, oxygen concentrations remain close to atmospheric saturation due to gas exchange and photosynthetic production by phytoplankton. As organic matter sinks and is re-mineralized in subsurface waters, oxygen is consumed, giving rise to vertical gradients. However,

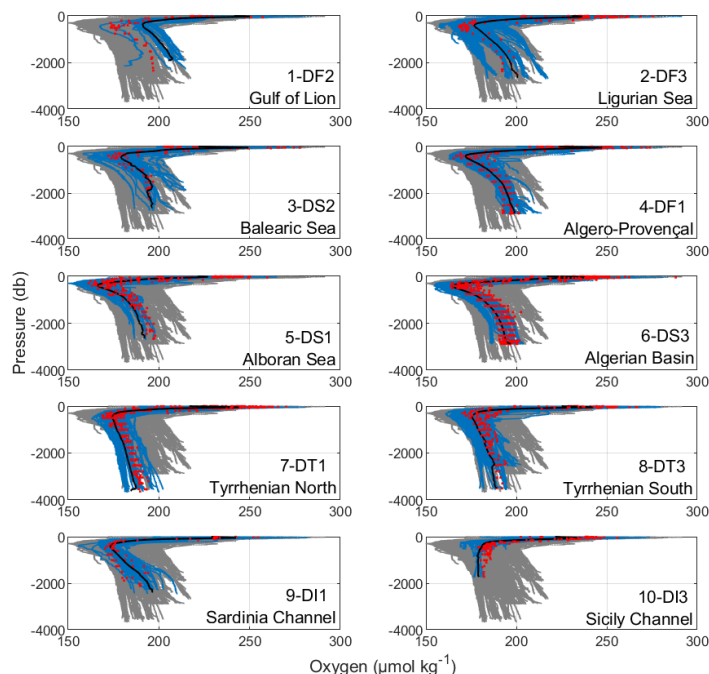
unlike any other ocean basins where pronounced Oxygen minimum zone develops, the WMED remain relatively well-oxygenated owing the periodic deep convection events in the Gulf of Lion (DF2) which generate the WMDW. This dense, oxygen -rich water mass ventilates deep layers across subregions such as the Algerian (DS3, DF1), Ligurian (DF3) and Gulf of lion (DF2) which are known to be among the most ventilated areas (Schneider et al., 2014).

To provide a comprehensive view of this oxygen distribution, Fig. 4a presents the vertical CTD oxygen profiles versus pressure across ten WMED subregions defined in Fig.4b, alongside data from reference cruises (Table 2). The blue shading highlights the oxygen concertation range within each subregion, revealing clear spatial differences across depth layers. one recurring feature is the intermediate depth oxygen minimum layer (OML), typically found between 300 and 600 db. This layer corresponds to the core of the LIW, which is warmer, saltier, and consistently lower in oxygen compared to surrounding water (Tanhua et al., 2013; Coppola et al., 2018; Mavropoulou et al., 2020). The depth, thickness, and intensity of the OML vary regionally and interannually, influenced by remineralization rates, nutrient availability, mixing intensity and regional circulation (Coppola et al., 2018). In the Tyrrhenian subregion, the OML is followed by increasing Oxygen concentrations at depth, suggesting downward diffusion of more oxygenated water. In contrast, the lowest oxygen concentrations in the WMED are observed in the Sicily channel and Tyrrhenian Sea, where the LIW is prominent and deep ventilation is weal. Meanwhile on the Alboran and Balearic seas exhibit relatively well(oxygenated profiles through the water column, a result of both the influence of the WMDW and enhanced vertical fluxes driven by mesoscale and sub-mesoscale processes that transport oxygen-rich surface water downward (Middleton et al., 2025).

The vertical distribution of dissolved Oxygen in the WMED exhibits a distinct pattern across different depth layers as illustrated in the vertical profiles shown in Fig.3(a). These profiles, which span ten subregions, provide a comprehensive view of spatial coverage, considering the depth component in conjunction with the reference dataset.

Broadly speaking, profiles reveal a general trend of high concentrations in both the upper and bottom layers, with an intermediate oxygen minimum layer, typically observed between 400 and 600 meters (Mavropoulou et al., 2020). At greater depths, subregions exhibit distinct behaviors. The dissimilarities in the vertical distribution highlight regional variations, influenced by factors such as circulation patterns, biological activity, and the unique physical characteristics of each region. This is particularly true for the Mediterranean, characterized by a complex circulation pattern involving inflows from the Atlantic Ocean, surface currents, and deep water formation. Circulation patterns play a crucial role in transporting oxygen rich or oxygen-poor water masses to different regions (Mavropoulou et al., 2020). For instance, in Figure 3a the DF2 Gulf of Lion, oxygen-rich waters reach the deep WMED by means of winter deep convection.

(a)



(b)

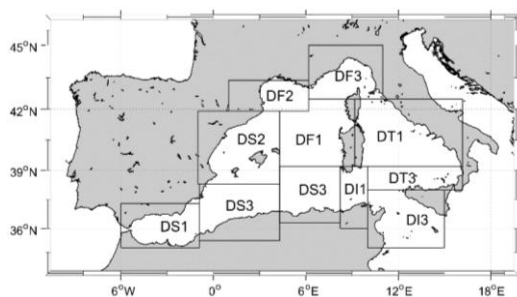


Figure 43. (a)

(a) Overview of CTD oxygen distribution versus pressure for the WMED in grey, from the original dataset after the initial quality control (1st QC). The blue represents the vertical distribution within each subregion (refer to Table S1). The black lines denote the mean profile of each subregion over the entire period. The red dots denote the reference data. (b) Geographical map indicating the geographical limits from MEDAR/Medatlas sub-regions (defined in Table S1, adapted from Manca et al. (2004)).

Vertical profiles of oxygen distribution for the entire WMED in grey, from the original dataset after the initial quality control (1st QC). The blue represents the vertical distribution within each subregion (refer to Table S1). The black lines denote the mean profile of each subregion over the entire study period. The red lines represent the reference data for each region. (b) Geographical map of the WMED indicating the geographical limits from MEDAR/Medatlas sub-regions (defined in Table S1). Adapted from Manca et al. (2004).

3 Quality control methods

3.1 Primary quality control of CTD-O2 data

Each cruise was converted to standard units. The GSW toolbox was used to calculate conservative temperature (CT), absolute salinity (SA), and potential density. Dissolved oxygen was converted from milliliters per liter (ml L⁻¹) to micromoles per kilogram (μmol kg⁻¹) using potential density and the conversion factor 44.66 to ensure uniformity. Then each cruise went through a rigorous scan for outliers, each parameter was assigned a data quality flag. Initially set to 2 for acceptable values, flag 3 for questionable values and to 9 for data following WOCE. However, the cruises did not necessarily have all parameters analyzed to the highest standards, and insufficient metadata. There often are insufficient deep stations to compare data with reference data. The primary quality control (1st QC) procedure involved the identification of outlier profiles and/or data points in each cruise. Outliers were flagged, indicating the quality of each value (refer to Table 3 in Belgacem et al., 2020). Flagging was specific to the precision of each parameter for each cruise. Property-property plots were examined for each region, and values identified as outliers in more scatter plots were flagged as questionable. Approximately 0.2% of CTD O2 data were considered outliers and flagged as 3. The 1st QC can be subjective, as it relies on the expertise of the individual inspecting the data.

To assess the internal consistency and precision of the CTD oxygen data across cruises, we computed Median and median absolute deviation (MAD) of deep oxygen concentrations (>800 dbar, as summarized in Fig.6 and Table S3, in supplementary) to sidestep any variability associated with atmospheric forcing or mesoscale variability and residual outliers.

Figure 5 (a) highlights the spatial variability in deep-water oxygen concentrations across the WMED. A distinct east-west gradient is evident, with lower oxygen levels (blue tones) characterizing the eastern subregions, including the Tyrrhenian Sea, Sardinia channel, and Sicily channel; in contrast, higher oxygen concentration (green to yellow) is observed in the westernmost regions, reflecting enhanced ventilation associated with deep convection processes in the Gulf of Lion. MAD was used as a proxy for precision, while comparisons of cruise-level medians with regional medians served to identify potential biases or systematic offsets.

Overall, MAD values ranges from 0.1 to 7.5 μmol/kg. in well-sampled subregions (≥5 cruises), high MAD or anomalous medians were used to recognize potentially problematic cruise.

In the Ligurian Sea (DF3), among five cruises, cruise #3 and #21 exhibited the highest MAD. While cruise 2, had a median consistent with other cruises, cruise #3 was ~10 μmol/kg lower, and cruise #6 was 1.6 μmol/kg higher, despite a low MAD. This discrepancy suggests potential bias or calibration issues, especially for cruise #6.

In the Balearic Sea (DS2), six cruises sampled the deep waters. All but cruises #3 and #6, showed low MAD. These two cruises had MADs of 5.4 and 6.9 μmol/kg, respectively, raising concerns about their precision.

In the Algéro-Provençal region (DF1), ten cruises sampled this subregion. Cruise #24 has the highest MAD (7.5 μmol/kg) and the highest median but was also based on only two profiles, likely explaining the high uncertainty. cruise #3 again showed an anomalously high median (197.6 μmol/kg), and cruise #6 has an elevated MAD of 4.2 μmol/kg.

Formatted: No bullets or numbering

Formatted: Font: (Default) +Headings CS (Times New Roman), 10 pt, Complex Script Font: +Headings CS (Times New Roman), 10 pt

Formatted: Font: (Default) +Headings CS (Times New Roman), 10 pt, Complex Script Font: +Headings CS (Times New Roman), 10 pt

In the Algerian basin (DS3), ten cruises showed generally good agreement (MAD between 1.8 and 4.1 $\mu\text{mol/kg}$), however, cruise #22 (2013) had an elevated oxygen value, potentially capturing a real increase in deep oxygen. In contrast, cruise #3 (2005), showed a regionally anomalous median, suggesting possible quality issues.

In the Tyrrhenian North region (DT1), with 14 cruises, this region has MADs from 1 to 4.5 $\mu\text{mol/kg}$. Cruises #3 and #22 displayed larger MADs and only cruise #3 had high median, while cruise #2 recorded the lowest deep oxygen concentrations.

In the Tyrrhenian South region (DT3), the most frequently sampled region (20 cruises), MADs ranged from 0.1 and 5.3 $\mu\text{mol/kg}$. elevated MADs were observed in cruise #2, #3, #5, #6, #10, and #24, suggesting noise.

In Sardinia Channel (DI1), fifteen cruises showed relatively consistent medians, but MAD values were generally higher (3.5 to 6.5 $\mu\text{mol/kg}$). Recent cruises, particularly cruise #24, showed the highest median (202.2 \pm 6.3 $\mu\text{mol/kg}$), significantly higher than earlier cruises, possibly indicating calibration issues.

Following the approach adapted from Olsen et al. (2016), large MADs combined with anomalous medians and limited spatial coverage (i.e., subregions) point to low internal precision and potential systematic error. Cruise #3 (multiple subregions) is consistently showing high MAD or biased medians. Cruise #6 (DF3, DS2, DT3) has an unusually high median in DF3 and high MAD in DS2 and DT3. Cruise #24 (DS3, DT1) is showing an elevated deep oxygen and large MAD, save for Cruise #22. Cruise #2 (DT1, DT3) show low median and high MAD, possibly indicating systematic error, same for cruise #5.

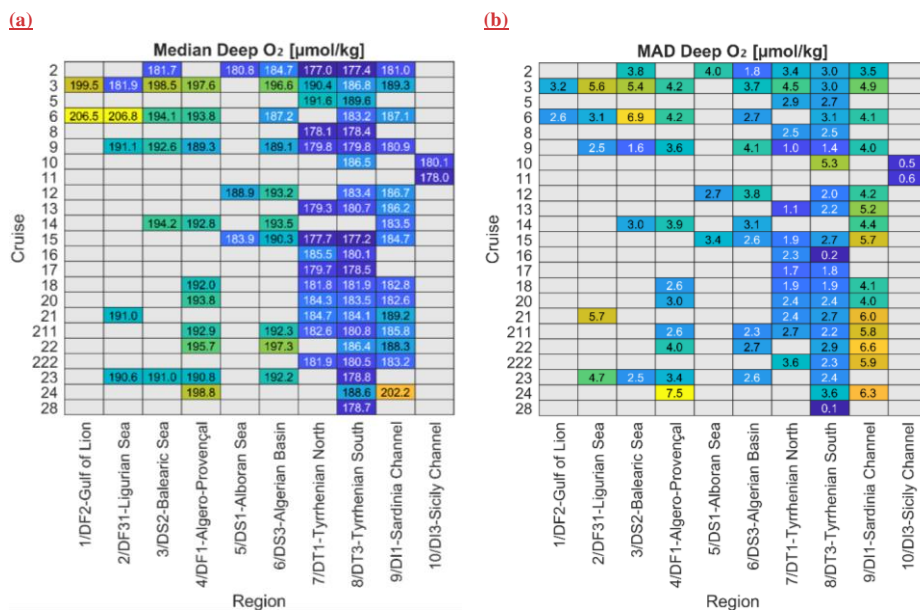


Figure 5. Median and MAD of deep CTD oxygen concentrations (>800 dbar). Heatmaps showing (a) the median and (b) the median absolute deviation (MAD) of CTD dissolved oxygen concentrations at pressure >800 dbar, organized by cruise (rows) and geographic subregion (columns). These metrics support the intercomparison of deep oxygen distribution and data quality across the CTDO2-WMED dataset. (Table S3).

314
315
316

Formatted: Font: (Default) +Headings CS (Times New Roman), 10 pt, Complex Script Font: +Headings CS (Times New Roman), 10 pt

Formatted: Normal, No bullets or numbering

Formatted: Font: (Default) +Body (Calibri), 11 pt, Not Bold, Complex Script Font: +Body CS (Arial), 11 pt, Not Bold, Not Italic, English (United States)

Formatted: Normal, Space After: 0 pt, No bullets or numbering

2.2 Reference data

The previously described CNR collection data is compared to deep water data collected in the same area (details are in section 3.2).

A total of six cruises have been identified (see Table 2) with documented high-quality dataset (Figure 4), collected in the Mediterranean Sea through international projects. Defined as “reference cruise,” they adhere to the recommendations of the World Ocean Circulation Experiment (WOCE) and the Global Ocean Ship-Based Hydrographic Investigations Program (GO-SHIP) protocols (Langdon 2010). Among these, cruises 06MT20011018 and 06MT20110405 are significant surveys, contributing to the GLODAPv2 dataset (Olsen et al., 2016), which facilitate comprehensive mapping of biogeochemical parameters.

During cruise both cruises, quality control procedures were applied to data, and minimal corrections to oxygen measurements were made, ensuring excellent data quality. Additional information regarding these cruises can be found in the work of Tanhua et al. (2013a) and Hainbucher (2012). For further details regarding these references, one can refer to the adjustment table available at <https://glodap.info/> (last access: August 2024) and the work by Olsen et al. (2020).

Similarly, cruises 48UR20070528 (TRANSMED-II) and 29AH20140426 (HOTMIX) which are related to CARIMED (CARbon, tracer and ancillary data In the MEDsea) that aims to be an internally consistent database containing inorganic carbon data relevant for this basin (Álvarez et al., in preparation); which means that this cruise underwent rigorous quality control processes

The TALPro cruises conducted in 2016 (Tanhua, 2019a, 2019b; Jullion, 2016) and in 2022 (Schroeder, 2022) are associated with the MedSHIP program, which follows the guidelines established by the international GO-SHIP initiative. This program is dedicated to high-quality data collection and analysis to evaluate the impacts of climate on marine environments (Schroeder et al., 2015, 2024).

Following the standards and charts of these programs, the quality of measurements obtained during these cruises has been ensured, demonstrating both precision and reliability, and thus used as reference cruises in the secondary quality control procedure described below in section 3.2.

Table 2. Overview of reference cruises utilized in the secondary quality control process with their Expocode and Identification number (ID). The data spans from 2001 to 2022.

ID	Common name	EXPOCODE	Date starts and end	Stations	Source	Chief scientist(s)
6	MSI/2	06MT20011018	18 Oct–11 Nov 2001	6	GLODAPv2	Wolfgang Roether
22	TRANSMED-LEGH	48UR20070528	28 May–12 Jun 2007	4	CARIMED	Maurizio Azzaro
64	M84/3	06MT20110405	5–28 Apr 2011	20	GLODAPv2	Toste Tanhua
17	HOTMIX	29AH20140426	26 Apr–31 May 2014	18	CARIMED	Javier Aristegui
27	TALPro-2016	29AJ20160818	18–28 Aug 2016	42	MedSHIP programme	Loïc Jullion, Katrin Schroeder
28	TALPro-2022	11BG20220517	17–26 May 2022	24	MedSHIP/ MedSHIP programme	Katrin Schroeder

Formatted: No bullets or numbering

Field Code Changed

Formatted: English (United States)

(a)

(b)

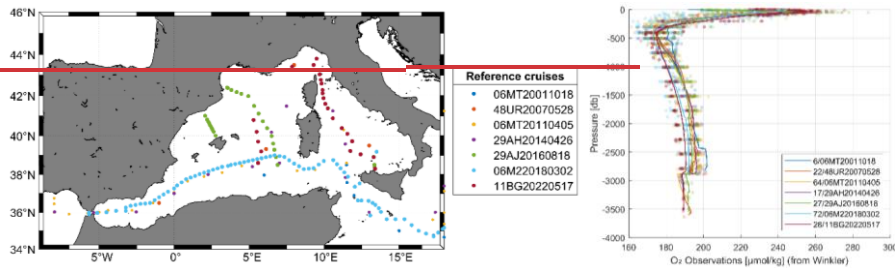


Figure 4. Reference cruises: (a) Map with stations. (b) Dissolved oxygen data from Winkler measurements and corresponding mean profile from the reference cruises.

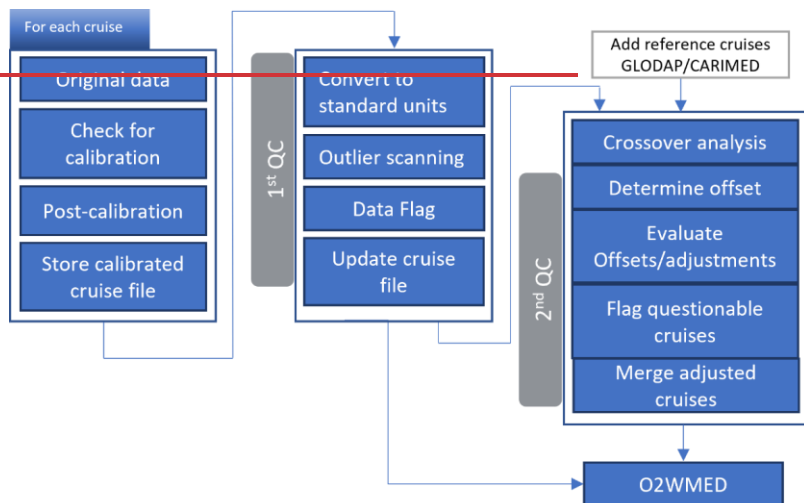


Figure 5. Flowchart illustrating the sequential steps from calibration through primary quality control (1st QC) to secondary quality control (2nd QC) and finally to O₂WMED.

3—Quality assurance methods

3.1—Primary quality control of O₂ CTD data

Following Figure 5 chart, each cruise variable was scanned for any spike before calibration. Then values were converted to standard units when needed. Dissolved oxygen was converted from milliliters per liter (ml L^{-1}) to micromoles per kilogram ($\mu\text{mol kg}^{-1}$) using potential density and the conversion factor 44.66 to ensure uniformity. For a thorough data integrity, each parameter was assigned a data quality flag. Initially set to 2 for acceptable values, flag 3 for questionable values and to 9 for data following WOCE.

The primary quality control (1st QC) procedure involved the identification of outlier profiles and/or data points in each cruise. Outliers were flagged, indicating the quality of each value (refer to Table 3 in Belgacem et al., 2020). Flagging was specific to the precision of each parameter for each cruise. Property-property plots were then

examined for each region, and values identified as outliers in more scatter plots were flagged as questionable (see Fig. 6).

A scatter plot depicting the oxygen distribution provided an overview, with values flagged as 3 for questionable values or 2 for accepted values. Approximately 0.19% of CTD oxygen data were considered outliers and flagged as 3. The 1st QC can be subjective, as it relies on the expertise of the individual inspecting the data.

The coefficient of variation of Oxygen profiles (CV, defined as standard deviation over mean) for each layer (surface: 0–250 db; intermediate: 250–1000 db; deep: below 1000 db) has been considered. CV in the surface layer (0–250 db, CV = 11.7%) were relatively high due large frequency variability (caused by air-sea interaction), at intermediate levels (250–1000db, CV = 4.5%), and deep layer (below 1000 db, CV = 4.4%), these variabilities are reduced.

3.2 Secondary quality control: crossover analysis

The secondary quality control (2nd QC) method involves comparing the CNR cruises with reference cruises. The reference data are assumed to be accurate, and stable, particularly in deep water; however, this assumption may not always be effective, for more recent cruises due to the region's strong spatial gradients and potential long-term changes in dissolved oxygen concentrations. In global data synthesis efforts such as GLODAP and CARINA, a 1% agreement threshold has been widely used in crossover analysis to detect potential biases and ensure consistency across cruises. However, this could don't be valid for the case of the Mediterranean Sea. These changes may affect the entire Basin in long-term, particularly the intermediate and deep water. Here, we check the consistency of the reference dataset, test and identify accuracy thresholds and identify the least variable depth range on which to apply the Xover analysis.

• Reference data:

The previously described CNR CTDO₂ profile data collection is compared to deep water observation from the same area. A total of seven cruises have been identified (Table 2, Figure 6) with documented high-quality dataset during which discrete oxygen measurements were collected in the Mediterranean Sea through international projects. Defined as “reference cruise,” they adhere to the recommendations of the World Ocean Circulation Experiment (WOCE) and the Global Ocean Ship-Based Hydrographic Investigations Program (GO-SHIP) protocols (Langdon 2010). Among these, cruises 06MT20011018 and 06MT20110405 are significant surveys, contributing to the GLODAPv2 dataset (Olsen et al., 2016). During these cruises, quality control procedures were applied, and minimal corrections to oxygen measurements were made, ensuring excellent data quality. Additional information regarding these cruises can be found in the work of Tanhua et al. (2013a) and Hainbucher (2012). For further details, one can refer to the adjustment table available at <https://glodap.info/> (last access: August 2024) and the work by Olsen et al. (2020).

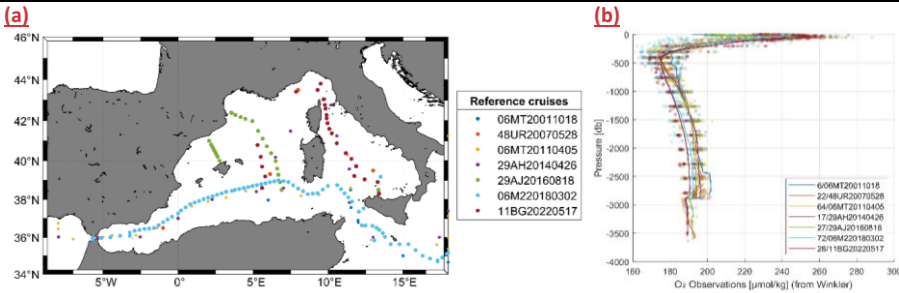
Similarly cruises 48UR20070528 (TRANSMED II), 29AH20140426 (HOTMIX) and 06M220180302 (MSM72) which are related to CARIMED (CARbon, tracer, and ancillary data In the MEDsea) that aims to be an internally consistent database containing inorganic carbon data (Álvarez et al., in preparation); which means that this cruise underwent rigorous quality control processes. The TALPpro cruises conducted in 2016 (Tanhua, 2019a, 2019b;

Formatted: Space After: 8 pt, Adjust space between Latin and Asian text, Adjust space between Asian text and numbers

Jullion, 2016) and in 2022 (Schroeder, 2022) are associated with the MedSHIP program, which follows the guidelines established by the international GO-SHIP initiative. This program is dedicated to high-quality data collection and analysis to evaluate the impacts of climate on marine environments (Schroeder et al., 2015, 2024). Following the standards and charts of these programs, the quality of measurements obtained during these cruises has been ensured, demonstrating both precision and reliability, and thus used as reference cruises in the 2nd QC. To sum-up, we are using these bottle oxygen reference from seven cruises to check and evaluate the CTD-O₂ sensor-based dataset.

Table 2. Overview of reference dataset utilized in the 2nd QC process with their Expocode and Identification number (ID). The data spans from 2001 to 2022.

ID	Common name	EXPCODE	Date starts and end	Stations	Source	Chief scientist(s)
6	<i>M51/2</i>	06MT20011018	18 Oct–11 Nov 2001	6	GLODAPv2	Wolfgang Roether
22	<i>TRANSMED_LEG II</i>	48UR20070528	28 May–12 Jun 2007	4	CARIMED	Maurizo Azzaro
64	<i>M84/3</i>	06MT20110405	5–28 Apr 2011	20	GLODAPv2	Toste Tanhua
17	<i>HOTMIX</i>	29AH20140426	26 Apr–31 May 2014	18	CARIMED	Javier Aristegui
27	<i>TAIPro-2016</i>	29AJ20160818	18–28 Aug 2016	42	MedSHIP programme	Loïc Jullion, Katrin Schroeder
72	<i>MSM72</i>	06M220180302	2 Mar–3 Apr 2018	130	Go-SHIP	Jens Karstens
28	<i>TAIPro-2022</i>	11BG20220517	17–26 May 2022	24	MedSHIP programme	Katrin Schroeder



(c)

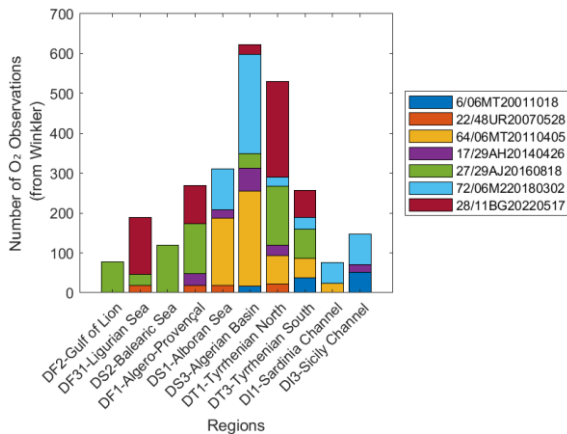


Figure 6. Reference cruises: (a) Map with stations. (b) Dissolved oxygen data from Winkler measurements and corresponding mean profile from the reference cruises and (c) Number of oxygen observations in the reference for each region.

Figure 6 (c) presents a histogram of the regional distribution of the reference dataset, which aligns well with CTDO2-WMED dataset, both datasets consistently highlight the Tyrrhenian (DT1) and the Algerian basin (DS3) as the most frequently sampled subregions over the multiple years.

To evaluate the precision of each cruise data, adjacent profiles were compared. Standard deviations and averages were calculated for deep layers (depths greater than 1000 dbar, as shown in Table 3) to sidestep any variability associated with atmospheric forcing or mesoscale patterns.

Data with poor precision are expected to show large standard deviations, indicating significant discrepancies from nearby measurements.

Additionally, this analysis provides an overview of oxygen content in deep layers and the spatial extent of measurements for each survey. Following the subdivision of the WMED proposed by Manca et al. (2004) (see Fig. 3b and Table S1), comparison of regional averages allowed the identification of potentially suspect cruises.

The standard deviation between cruises in deep layers varied between 0.5 and 7.6 $\mu\text{mol kg}^{-1}$. Overall, profiles collected in close proximity exhibit similar variability.

The lowest standard deviations were observed in data collected from the Sicily Channel (DI3) subregions during cruises no. 10, no. 11, and no. 211, indicating high data quality for these surveys.

433 Fifteen surveys were conducted in Sardinia Channel (DI1), all displaying similar variability. Standard deviation
434 among cruises in this region ranged between 4 to 6.5 $\mu\text{mol kg}^{-1}$, demonstrating good agreement amid
435 measurements.

436 A similar pattern was observed in the Tyrrhenian South region (DT3), which was samples by 22 cruises.

437 The lowest average was recorded during cruise #2, which was lower than neighboring cruises, while cruise #24
438 exhibited the highest average; however, the standard deviation did not show significant variation.

439 In the Tyrrhenian North region (DT1), eighteen cruises were conducted, with standard deviations ranging from 1.4
440 to 5.5. Notably, cruise no. 3 displayed a larger standard deviation of 7.5 $\mu\text{mol kg}^{-1}$.

441 In the Algerian basin (DS3), ten cruises were conducted, yielding standard deviations between 3.3 and 4.4 μmol
442 kg^{-1} , similar to the findings in the Alboran Sea (DS1).

443 In the Algéro-Provençal region (DF1), we find data from eleven cruises, with the highest standard deviations
444 recorded during cruises no. 3 and no. 24.

445 In the Balearic Sea (DS2), six cruises sampled the deep layer, all exhibiting low standard deviations, except for
446 cruises #3 and #6, which had values of 6.1 and 7.6 $\mu\text{mol kg}^{-1}$ respectively.

447 In the Ligurian Sea (DF3), five cruises where conducted, with cruise no.3 displaying anomalous behavior
448 characterized by a high standard deviation and average compared to neighboring cruises, indicating that the data
449 from cruise #3 were higher the nearby measurements.

450 High standard deviations suggest extensive spatial coverage, as seen in cruises no. 3, no. 6, no.12 and no.15, while
451 low standard deviation, such as in cruise no. 11 (DI3-Sicily Channel), no. 17, and no. 8 (predominantly in DT1-
452 Tyrrhenian North and DT3-Tyrrhenian South), suggests smaller spatial coverage.

453 The condition suggested by Olsen et al. (2016), which suggests that large standard deviation coupled with narrow
454 spatial coverage implies imprecise data, was not found in our dataset.

455 An examination of data spread across various regions revealed that some cruises exhibited large standard
456 deviations compared to nearby profiles. For instance, cruise no.3 (Tyrrhenian North, Balearic Sea and Ligurian
457 Sea) had standard deviations exceeding 6.1 $\mu\text{mol kg}^{-1}$, suggesting that this cruise was less precise than the others
458 conducted in the same region.

459 Comparing deep profiles provided evidence regarding data precision; uncertainties in measurements may
460 complicate decisions about the adjustments proposed by the 2nd QC phase.

461 Cruises no. 25, no. 27, no. 28 did not include data below 1000 dbar; however, these datasets underwent quality
462 checks and are included in the final dataset.

463 **Table 3. Average and standard deviation (STD) of CTD dissolved oxygen by cruise and for each region deeper than**
464 **1000 db.**

Cruise ID	EXPCODE/ region	Regional avg CTD OXY ($\mu\text{mol kg}^{-1}$)	STD CTD OXY ($\mu\text{mol kg}^{-1}$)
2	48UR20041006/ DS2-Balearic Sea	182.48	4.193 3.27

Formatted: English (United States)

Formatted: English (United States)

	DS1-Alboran-Sea	181.71	3.59
	DS3-Algerian-Basin	183.59	3.32
	DT1-Tyrrhenian-North	177.49	3.21
	DT3-Tyrrhenian-South	177.57	3.09
-	DH-Sardinia-Channel	181.02	4.17
3	48UR20050412/		9.538
	DF2-Gulf-of-Lion	199.65	5.64
	DF3-Ligurian-Sea	183.42	7.46
	DS2-Balearic-Sea	200.67	6.15
	DF1-Algero-Provençal	197.87	5.76
	DS3-Algerian-Basin	196.17	4.44
	DT1-Tyrrhenian-North	191.03	4.67
	DT3-Tyrrhenian-South	189.31	4.13
-	DH-Sardinia-Channel	191.27	4.68
5	48UR20051116/		3.542
	DT1-Tyrrhenian-North	191.73	2.79
-	DT3-Tyrrhenian-South	190.22	3.90
6	48UR20060608/		9.76
	DF2-Gulf-of-Lion	207.71	3.09
	DF3-Ligurian-Sea	207.72	3.85
	DS2-Balearic-Sea	195.00	7.60
	DF1-Algero-Provençal	194.82	4.95
	DS3-Algerian-Basin	187.81	3.75
	DT3-Tyrrhenian-South	185.06	3.49
	DH-Sardinia-Channel	188.80	4.21
8	48UR20060928/		2.812
	DT1-Tyrrhenian-North	177.87	2.81
	DT3-Tyrrhenian-South	178.15	2.80
9	48UR20071005/		5.77
	DF2-Gulf-of-Lion	185.57	1.38
	DF3-Ligurian-Sea	190.87	3.37
	DS2-Balearic-Sea	193.20	1.61
	DF1-Algero-Provençal	189.95	4.01
	DS3-Algerian-Basin	189.55	4.16
	DT1-Tyrrhenian-North	179.48	1.41
	DT3-Tyrrhenian-South	180.09	2.18
	DH-Sardinia-Channel	183.39	4.15
10	48UR20080318/		5.079
	DT3-Tyrrhenian-South	187.15	4.72
-	DH-Sicily-Strait	180.18	0.72
11	48UR20080905/		0.610
-	DH-Sicily-Channel	177.74	0.61
12	48UR20081103/		4.81
	DF1-Algero-Provençal	192.51	4.04
	DS1-Alboran-Sea	190.61	3.17
	DS3-Algerian-Basin	193.71	3.81
	DT3-Tyrrhenian-South	184.63	3.14
-	DH-Sardinia-Channel	188.58	4.53
13	48UR20090508/		3.044
	DT1-Tyrrhenian-North	180.42	1.59
	DT3-Tyrrhenian-South	181.78	2.83
	DH-Sardinia-Channel	187.67	4.75
14	48UR20100430/		5.44
	DS2-Balearic-Sea	194.39	3.15
	DF1-Algero-Provençal	192.67	4.69
	DS3-Algerian-Basin	193.28	3.55
	DT1-Tyrrhenian-North	184.26	2.23
	DT3-Tyrrhenian-South	183.86	2.02
	DH-Sardinia-Channel	186.52	5.23
15	48UR20100731/		6.21
	DS1-Alboran-Sea	186.58	3.68
	DS3-Algerian-Basin	189.94	3.34
	DT1-Tyrrhenian-North	178.03	2.22
	DT3-Tyrrhenian-South	178.14	3.27
	DH-Sardinia-Channel	186.60	5.18
16	48UR20101123/		3.96
	DT1-Tyrrhenian-North	186.29	3.86
	DT3-Tyrrhenian-South	181.04	1.68
17	48UR20110421/		2.47
	DT1-Tyrrhenian-North	180.0	1.86
	DT3-Tyrrhenian-South	179.4	2.80
18	48UR20111109/		5.62
	DF1-Algero-Provençal	191.20	3.92
	DT1-Tyrrhenian-North	182.00	2.22
	DT3-Tyrrhenian-South	182.79	3.15

Formatted: Space After: 8 pt, Line spacing: Multiple 1,08 li

	DI1-Sardinia-Channel	185.19	5.43
20	48UR20120111//		5.29
	DF1-Algero-Provençal	192.90	4.35
	DT1-Tyrrhenian-North	184.69	3.06
	DT3-Tyrrhenian-South	184.17	2.88
	DI1-Sardinia-Channel	186.06	5.60
21	48UR20121108//		5.73
	DF3-Ligurian-Sea	197.73	5.27
	DT1-Tyrrhenian-North	190.86	3.05
	DT3-Tyrrhenian-South	189.89	2.85
	DI1-Sardinia-Channel	196.25	5.42
21+	48UR20130604//		6.086
-	DF1-Algero-Provençal	192.907	4.337
-	DS3-Algerian-Basin	191.516	4.118
-	DT1-Tyrrhenian-North	183.228	3.139
-	DT3-Tyrrhenian-South	182.148	3.147
-	DI1-Sardinia-Channel	186.594	5.264
-	DI3-Sicily-Channel	178.630	0.531
22	48UR20131015//		6.03
	DF1-Algero-Provençal	195.96	4.90
	DS3-Algerian-Basin	196.54	4.24
	DT1-Tyrrhenian-North	188.79	4.38
	DT3-Tyrrhenian-South	187.66	3.92
	DI1-Sardinia-Channel	190.87	6.03
222	48QL20151123//		4.27
-	DT1-Tyrrhenian-North	183.17	3.84
-	DT3-Tyrrhenian-South	181.97	3.17
-	DI1-Sardinia-Channel	185.91	5.48
23	48QL20150804//		5.79
	DF3-Ligurian-Sea	190.75	4.91
	DS2-Balearic-Sea	191.13	3.21
	DF1-Algero-Provençal	190.32	4.43
	DS3-Algerian-Basin	191.41	3.85
	DT1-Tyrrhenian-North	184.60	3.60
	DT3-Tyrrhenian-South	180.45	3.24
24	48QL20171023//		7.195
	DF1-Algero-Provençal	200.42	6.49
	DT1-Tyrrhenian-North	193.62	5.53
	DT3-Tyrrhenian-South	190.62	4.26
	DI1-Sardinia-Channel	201.79	6.59
25*	48DP20180918//		
	DI3-Sicily-Channel	-	-
27*	48DP20221015//		
	DI3-Sicily-Channel	-	-
28*	48DP20230324//		
	DI3-Sicily-Channel	-	-

*Cruises not included in the second QC. In bold: the overall standard deviation by cruise; in normal font: regional standard deviation by cruise.

- Accuracy envelope in the WMED

To explore the feasibility of applying a broader accuracy threshold specific to the WMED, we assess whether relaxing the accuracy threshold to 2% is appropriate for the reference cruises in DS3 and DT1, two regions representative of contrasting deep-water dynamics.

For this analysis, each DO profiles from selected reference were interpolated to a standard pressure grid (0 - 3600 dbar) using a piecewise cubic Hermite interpolating. Mean DO profiles were then computed per cruise and averaged across cruises to produce a composite profile for each region (Fig.8).

Both subregions display the typical WMED oxygen structure as described in section above. However, the degree of interannual variability differs substantially between the two.

In the DT1 (Tyrrhenian Sea), oxygen profiles from different reference cruises show minimal variability between 800 and 2500 db, suggesting stable deep-water conditions. The Tyrrhenian deep waters are known to be ventilated not primarily by deep convection but through lateral advection and double-diffusion process (Durante et al., 2009).

Signs of episodic ventilation, particularly in 2007 and 2016 have been identified and discussed by Li and Tanhua (2020). The consistent/ slow increase in oxygen below 800 db likely reflect the influence of such processes, which may also explain the weak development of a well-defined tracer minimum zone (TMZ) in this region.

In contrast, DS3 (the Algerian basin) shows significantly more variability. While the overall profile shape is consistent, DO concentrations below 1500 db in recent cruises (2018 and 2022) are lower by 4-5 $\mu\text{mol/kg}$ compared to earlier cruises. These differences correspond to deviations of 2 to 4%, likely linked to temporal changes that may be linked shifts in deep water formation. Studies using transient tracers, have reported enhanced ventilation between 2001 and 2016. Consistent with our observations. However, as suggested by Li & Tanhua (2020), the declining intensity of deep convection in recent years has reduced oxygen renewal at depth, a trend clearly evident in DS3- Algerian basin, but not observed in the DT1- Tyrrhenian Sea, as also noted by Schneider et al. (2014)

Figure 7 (a,b) confirm the contrasting DO patterns between the two subregions, while , while zoomed panels (c) and (d) highlight the spread among cruises. The greater variability in DS3 supports the need to relax the 2nd QC threshold from 1% to 2% to accommodate natural variability rather than forcing potentially misleading corrections.

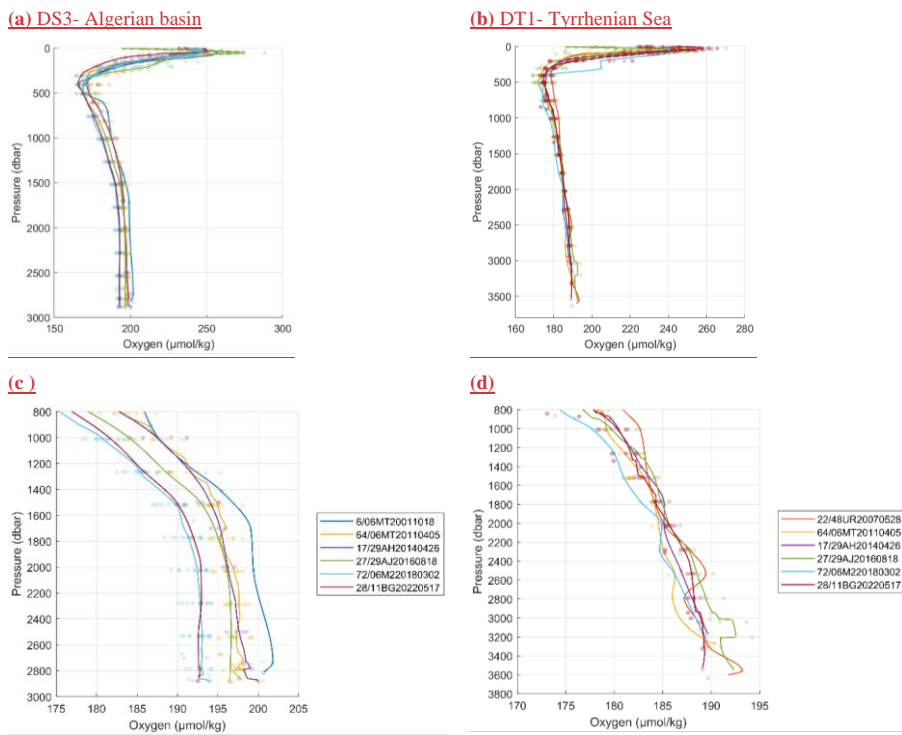


Figure 7. Average vertical profiles of dissolved oxygen in (a) the Algerian Basin and (b) the Tyrrhenian Sea. Panels (c) and (d) provide a zoomed view of the deep layers below 800 db. Colored dots represent individual oxygen sample, color-coded by cruise, while the solid-colored lines show the cruise-specific average profiles.

- Defining a stable pressure range for crossover analysis

497 To assess consistency in the deep layer of the reference dataset, we computed pairwise ratios (A/B) of average
498 dissolved oxygen between the tested cruise (e.g., A:6/06MT20011018) and the six reference cruises (B), the results
499 are shown in Figure 8 and Figure S1-2S.

500 In DS3 (Algerian basin), 29.7% of pairwise ratio fall within 1%, and 60.5% within 2%, while 39% exceed the 2%
501 threshold, highlighting higher variability compared to DT1(Tyrrhenian Sea), where 71.7% of ratios lie within 1%,
502 and 98.7% within 2%, indicating more stable deep-water conditions. Most discrepancies in both regions occur
503 below 2500 db where data are sparser and naturel variability increases.

504 Cruise 72(2018) and 28 (2022) in DS3 consistently show 2-4% lower oxygen than earlier cruises (64, 17, 27),
505 suggesting long-term decrease in oxygen or episodic variability. These patterns align with Gregoire et al.(2023)
506 and personal communication with L.Coppola, who attributed the 2022 anomaly to reduced deep convection. The
507 regionally stable layer across cruises lies between 800 and 2000 db, where interannual variability is minimal. This
508 depth range aligns with tracer minimum zone described by Li and Tanhua (2020), which reflects shifting
509 ventilation intensity over time. Given our dataset spans 2001/ 2004-2023 , a broader 800-2000 db is proposed for
510 crossover analysis to account for temporal and spatial changes.

511 This assessment follows secondary quality control procedures in the WMED; by adopting a 2% threshold, more
512 appropriate than 1% standard used in CARINA and GLODAP; we minimize the risk of applying unjustified
513 corrections to CTD oxygen data and accommodate the natural change in the region.

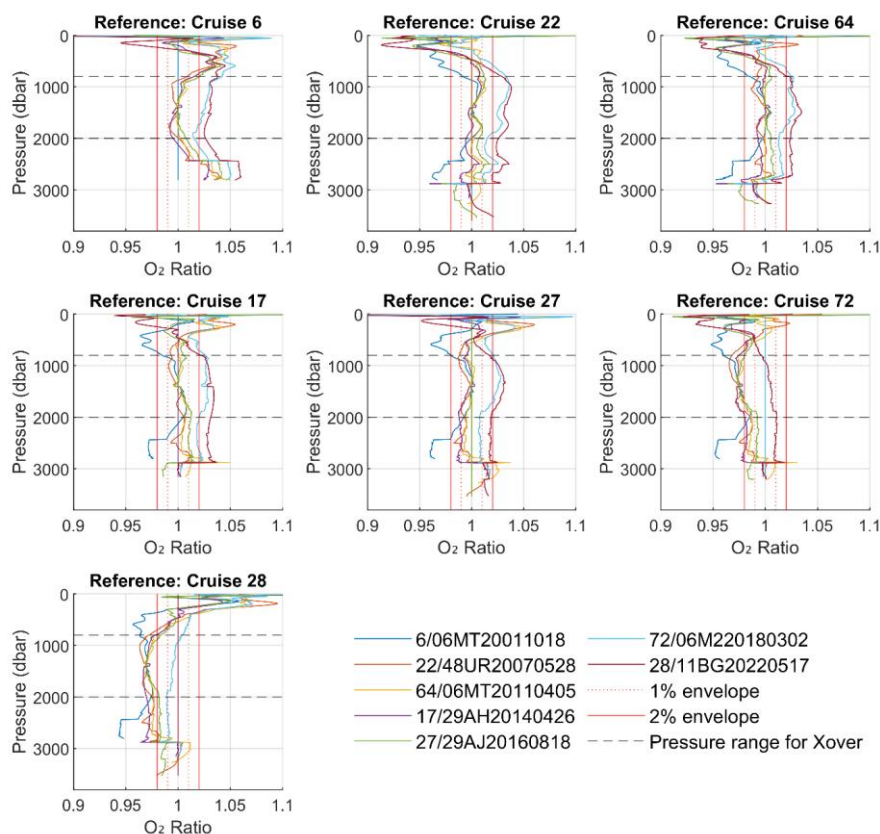


Figure 8. Vertical distribution of the ratio between the tested reference cruise (top of each subplot) vs the other references (in the legend box below). red continuous vertical line refer 2% accuracy envelope and red dashed line refer to 1% envelope to . Similar composite figures are in supplement for subregions DT1 (Fig. S1) and DS3 (Fig. S2) (zoom: 800-2000 dbar)

3.2 Secondary quality control: crossover analysis

The secondary quality control (2nd QC) method involves comparing the CNR cruises with reference cruises, as described in Section 2.2. The reference data are considered to be accurate, precise and stable, particularly in deep water; however, this assumption may not always be effective, especially for recent cruises. There is a notable lack of comprehensive studies addressing the general trends of dissolved oxygen levels in the Mediterranean Sea.

Consistency of the reference data:

Each profile from the reference cruises (see Table 2) was interpolated using a piecewise cubic Hermite interpolating scheme to standard pressure values ranging from 0 to 3600 dbar. Subsequently, all profiles were averaged to produce a single profile for each cruise in DS3 (Algerian Basin) and DT1 (Tyrrhenian). Figure XX shows the averaged vertical profiles in DS3 and DT1;

eventTable. Datastats > 1000 db for each region.

DS3				DT1		
Cruise #	RANGE	STD	OBS	RANGE	STD	OBS
6	14.1	5.27	7	NaN		
22	NAN			10.51	3.18	10
64	17.2	3.78	100	11.24	2.74	29
17	15.91	4.05	22	6.93	2.61	6
27	12.92	4.39	17	15.8	3.97	46
72	16	4.24	104	11.7	3.89	11
28	11.4	3.73	11	11.13	3.33	62

Figure XX illustrates the ratio (A/B) estimates between the tested cruise (A:6/06MT20011018) and the remaining six reference cruises (B).

Figure (a,b) agree about the DO type vertical profile, in the WMED. Which is quick a decrease in DO with depth to reach its minimum at 300 to 450db, then below 500db, DO increase slowly to each a local maxima at 1500db, and then remain constant. This is observed in DS3.

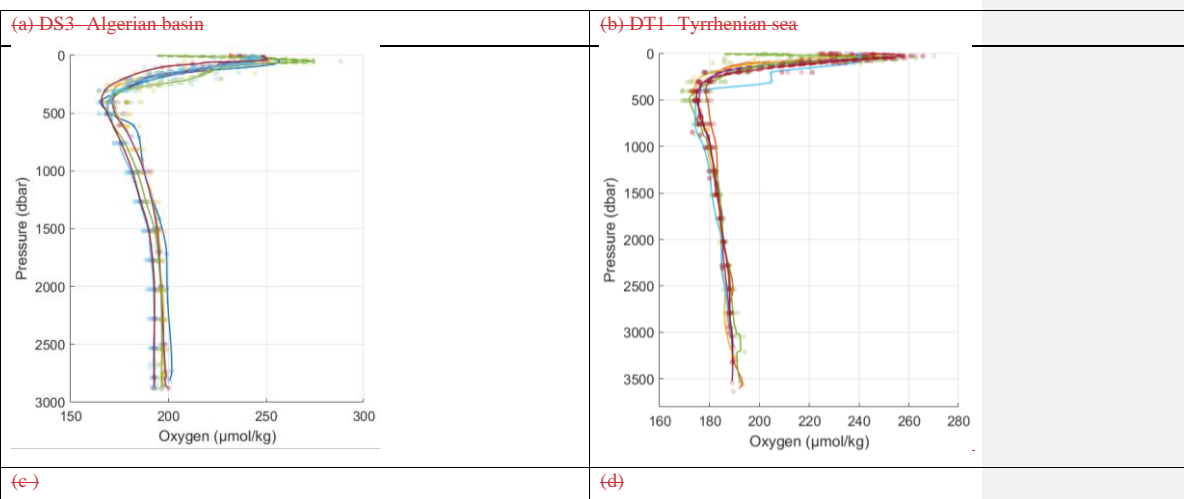
The difference in the Tyrrhenian, starts below 500 db, with a slow increase in DO with depth.

Looking at deeper layer, the Tyrrhenian show less variability and a compact relation between the different years, observed on the low standard deviation.

While , in the Algerian basin the overall variability is larger. Certainly this is due to the different circulation patterns in both areas.

We note a temporal change as well at deeper layers, in DS3, recent year cruise 2022 and 2018, were lower than previous years. exhibited Oxygen levels approximately 4% lower than those of the other years, as shown in

Fig.4(b)



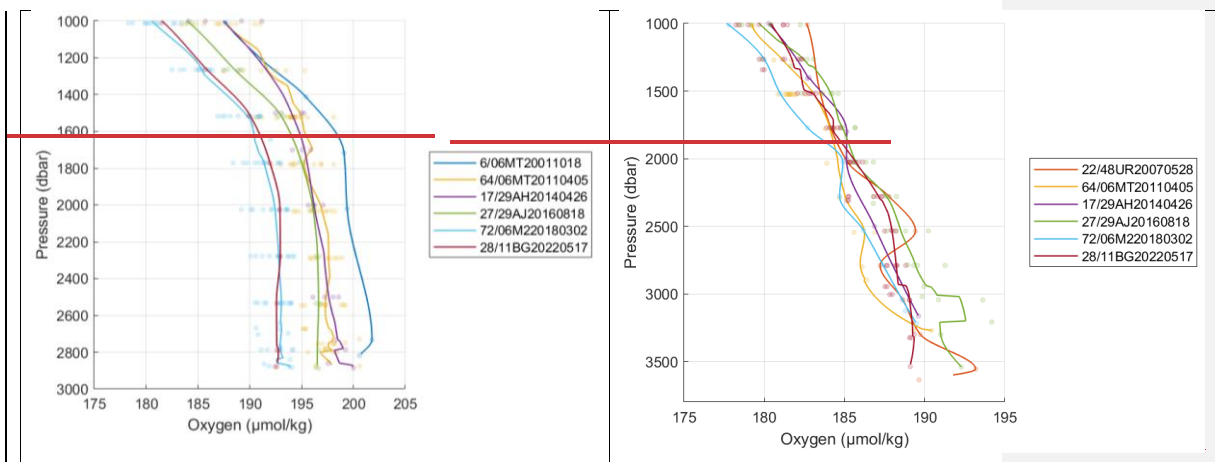


Figure: average vertical profiles of DO in (a) the Algerian Basin and (b) in the Tyrrhenian Sea. (c) and (d) are the zoom at pressure > 1000db. Dots are the DO samples color coded with cruise name, the standards deviation range in both lower panel (c, d) shows #cruise code = range (nb profiles), if a cruise does not have a range that means it has one profile in the subregion.

Table: Datastats > 1000 db for each region.

Cruise #	DS3				DT1		
	RANGE	STD	OBS		RANGE	STD	OBS
6	14.1	5.27	7		10.51	3.18	10
22	NAN				11.24	2.74	20
64	17.2	3.78	100		6.93	2.61	6
17	15.01	4.05	22		15.8	3.07	46
27	12.93	4.39	17		11.7	2.89	11
72	16	4.24	104		11.13	3.33	62
28	11.4	3.73	11				

Formatted: English (United States)

To asses consistency across cruises, we computed the pairwise ratios (A/B) of average DO values between the tested cruise (A:6/06MT20011018) and the remaining six reference cruises (B).

In DT1, 71.7% of ratios fell within 1%, and 98.7% fell within 2%, indicating strong agreement and low temporal variability. Only 1.3% of ratio values exceeded the 2% threshold, primarily below 2500 db, whenre the natural variability increases and the fewer observations at this level.

In DS3, however, this picture is more complex

We are aware of the spatial variability in the WMED and the south to north oxygen gradient, the comparison between the different cruises is focused on intermediate and deep layers, aims at identifying common range of

variability of these layers. This is an evaluation of variability range at intermediate and deep layers in Oxygen levels in time.

Based on the regional distribution of the reference O₂ observation of each reference cruise, we evaluate the accuracy envelope within the two most sampled subregions the Algerian Basin (DS3) and the Tyrrhenian sea (DT1).

To fairly quantify this difference between the different reference cruises in both regions, and to define the adequate accuracy envelope, Figure XX illustrates the ratio (A/B) estimates between the tested cruise (A: 606MT20011018) and the remaining six reference cruises (B):

This layer is characterized by lower temporal variability; thus, any change occurring between 1000 db and 2500 db do not significantly impact the results of the 2nd QC.

REGION DT1

Figures DT1 ratio avg show the ratio between all reference cruises within each other. All Cruises, show a good agreement in the variability patterns between 1000–2500db, falling in the 2% range (red continuous vertical lines), while we notice below 2500, the difference tends to be higher, giving evidence about the deeper status in oxygen content is not steady.

The results below indicate as well, a reduced variability below 1000 db, in DT1 tyrrhenian sea 71.7 % of the averaged ratio is within 1% and that 98.7% of the averaged ratio fall within the 2% envelope (including the 1%) indicating good agreement among the cruises, while 1.3% were outside the 2% envelope.

In the Algerian Basin (DS3), the difference between years is much larger, as observed above in the averaged profiles, the ratio below 1000db shows that cruises 72(2018) and 28/11BG20220517 were on average 2.4 % (with cruises 64(2011)) to 4% (with 2001, 17(2014), and 27(2016), lower than previous years. These particular cruises exhibited Oxygen levels approximately ~ 2 to ~ 4% lower than those of the other reference cruises, as shown in Fig. 4(b). Observations from these cruises, conducted in 2018 and 2022, may indicate natural variability in oxygen levels, suggesting a potential decline in the deep oxygen levels in the WMED, similar to trends observed in other oceanic regions (Grégoire et al., 2023). However, it is important to consider that this discrepancy could also stem from the precision of the Winkler titration values and their standardization with potassium iodate (KIO₃). A 4% difference in oxygen concentration is substantial and raises questions about the validity of such variation at these depths. personal communication with PI of the Winkler measurements agreed about the natural variability, and that 2022 could be a low oxygen event explained by the slowing down of the deep convection in the Gulf of Lion (L. Coppola, personal communication) adding to this cruise 2018 showed similar increment.

Not all cruises fall within the 2% envelope, especially recent ones in this region. The profile seems to show similar vertical distribution patterns in all cruises, below 2500 db, we notice a change. Overall, in DS3 algerian basin, we found that 29.7% of the pairwise averaged ratio are within 1%, and if we enlarge that range to 2%, we find that 60.46% of the values are within the 2% envelope, and that around 39% were outside the 2% range. In this region there is a consensus agreement similar to the one found in DT1 tyrrhenian that the majority of the ratio values of the pairwise reference cruises are within the 2% envelope.

595
596
597 ~~In this analysis, we assess the extent to which adjustments should be recommended. Following the standards~~
598 ~~established by CARINA and GLODAP data Atlantic observation based products, no adjustments smaller than 1%~~
599 ~~for oxygen measurements were applied (Hoppema et al., 2009), which does not fit to the WMED current status.~~
600 ~~Overall, in the Algerian region (DS3) three (64,17,27) out of six reference cruises demonstrated an average ratio~~
601 ~~below 1000 dbar, within the 1% accuracy limit (ranging from 0.99 to 1.01). two (72,28) out of six were within~~
602 ~~the 2%. While in the tyrrhenian sea (DT1), even though a continuous increased trend of Oxygen with depth is noted~~
603 ~~in all years of the reference cruises (figXX zoom DT1), the overall pairwise ratio was within the 1% envelope.~~
604 ~~That might be explained by the dynamic of the tyrrhenaian, its deeper layer is more stable then the Algerian basin~~
605 ~~, a subresion under the influence of many water masses newly formed since its oxygen is higher then the~~
606 ~~tyrrhenian. While older deep waters with lower oxygen levels reside in the tyrrhenian deep layers.~~

607 ~~To avoid any doubts and misleading evaluation of the bias whether from natural variability related to spatial~~
608 ~~variability or temporal changes or a real offset, the 2% reference envelope is set, which means no adjustment~~
609 ~~smaller then 2% for CTD oxygen is applied, adding to this a good agreement is perceived between 1000 and 2500~~
610 ~~m. The crossover analysis is performed at this range.~~
611
612
613
614
615
616
617
618
619
620

(a) (b) (c)

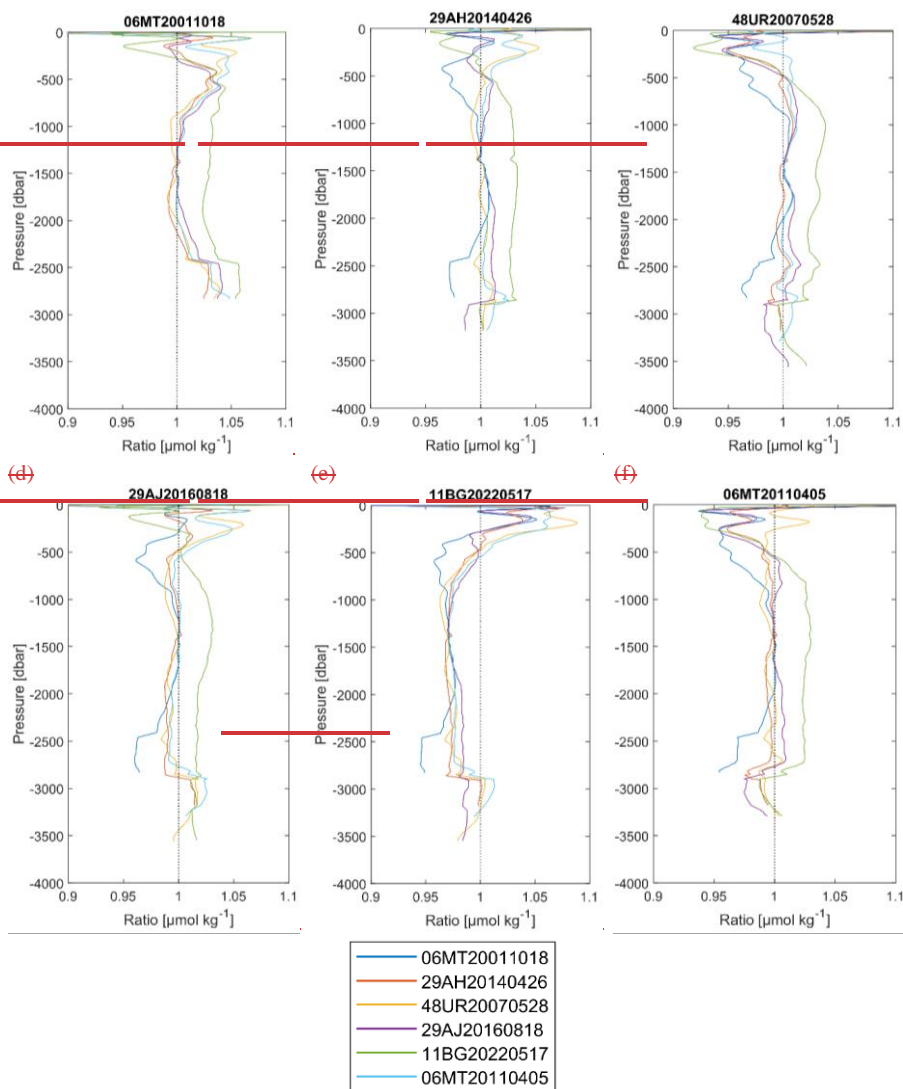


Figure 7. Vertical distribution of the ratio between the tested reference cruise (top of each subplot) vs the other references (in the legend box below).

Formatted: Normal

• Crossover analysis:

A crossover analysis, following the approach of Johnson et al. (2001), Tanhua et al. (2011) and Lauvset and Tanhua (2015), was conducted. Crossover analysis was run checking the cruises in the products versus the reference cruises. This analysis is predicated on the comparison of cruise pairs, where the differences between two cruises within a predefined spatial distance, here a radius of 2° latitude (approximately 222 km) are assessed. In this process, the interpolated profiles for each station in cruise C1 were compared to the interpolated profiles from cruise C2 within the specified maximum distance. A difference profile was generated for each pair of stations, with a minimum of three stations required for each crossover. Calculations were performed on density surfaces to ensure that data comparisons were made between the same or comparable water masses, thereby mitigating biases associated with variations in salinity.

Density values were calculated for each measurement, and data from each profile were interpolated using a piecewise cubic Hermite interpolating scheme to standard density levels. This iterative process was repeated for each station in the cruise, resulting in multiple difference profiles. The outcome is the weighted mean and standard deviation of the difference profiles for each cruise, referred to as the offset. The weighting applied to the profiles is based on their variability, giving higher importance to parts of the profiles with lower variability (adapted from Tanhua et al. 2010, 2015). This approach accommodates potential variability in deep layers, particularly in the Mediterranean Sea, which is influenced by ventilation processes (Testor et al., 2018).

Figure 8 illustrates an example of a crossover and offset between cruise pairs, while an overview of some crossovers vs. reference dataset are displayed in Section 4. All calculated offsets for each cruise were examined to determine the presence of any likely biases in the measurements.

Corrections were meticulously reviewed and justified whenever adjustments were deemed necessary (Table 4). It is important to note that high variability in deep water of the Mediterranean Sea, particularly in the Northern WMED where deep convection occurs, may increase the likelihood of detecting offsets in unbiased data.

The number of stations in the overlapping region (i.e., within the predefined radius) is critical for accurate offset estimation. For instance, as depicted in Figure 8 (a), 27 stations from C1 were compared to 15 stations from C2 to estimate the offset; a limited number of stations can introduce uncertainty into the offset estimate. Additionally, while the number of crossover cruises is significant, the Mediterranean Sea has a limited number of reference cruises available.

Following adjustments, the last step involves evaluation the overall internal consistency of the CNR-O2WMED using the weighted mean (WM) of the absolute offsets (D) of all crossovers (L) and the standard deviation (σ), following Tanhua et al. (2009) and Belgacem et al. (2020). This assessment quantifies the accuracy of the data product, as supported by previous studies (Hoppema et al., 2009; Sabine et al., 2010; Tanhua et al., 2009). Notably, our evaluation is based on offsets relative to a reference dataset, providing a comprehensive understanding of data consistency.

• Crossover analysis:

Commented [MB2]: Toste: Line 269: Section crossovers. I did not understand if you made a crossover analysis of all cruises vs. each other, or only the cruises in the product vs. the reference cruises. The text is not clear on that.

A crossover analysis, following the approach of Johnson et al. (2001), Tanhua et al., (2011) and Lauvset and Tanhua (2015), was conducted. Crossover analysis (Xover) was performed by checking the cruises CTDO2-WMED dataset to the reference cruises. The method is based on the comparison of cruise pairs, where the differences between two cruises within a predefined spatial distance, here a radius of 2° latitude (approximately 222 km) are assessed. The interpolated profiles for each station in cruise C1 were compared to the interpolated profiles from cruise C2 within the specified maximum distance. A difference profile was generated for each pair of stations, with a minimum of three stations required for each crossover. Calculations were performed on density surfaces to ensure that data comparisons were made between the same or comparable water masses, thereby mitigating biases associated with variations in salinity. Density values were calculated for each measurement, and data from each profile were interpolated using a piecewise cubic Hermite interpolating scheme to standard density levels. This iterative process was repeated for each station in the cruise, resulting in multiple difference profiles. The outcome is the weighted mean and standard deviation of the difference profiles for each cruise, referred to as the offset. The weighting applied to the profiles is based on their variability, giving higher importance to parts of the profiles with lower variability (adapted from Tanhua et al. 2010, 2015). In addition to conducting crossover analysis over the full spatial extent of each cruise, regional crossovers also performed using a modified clustering approach. In this method, clusters are manually defined based on predefined geographical subregions (Table S2); When sufficient profile coverage was available, analysis was focused on the most frequently sampled areas: the Tyrrhenian Sea (both DT1 & DT3), Algerian basin (DS3 & DF1) and the Alboran sea (DS1), as previously described. This regionalized approach helps reduce the likelihood of comparing stations influenced by distinct hydrographic regimes.

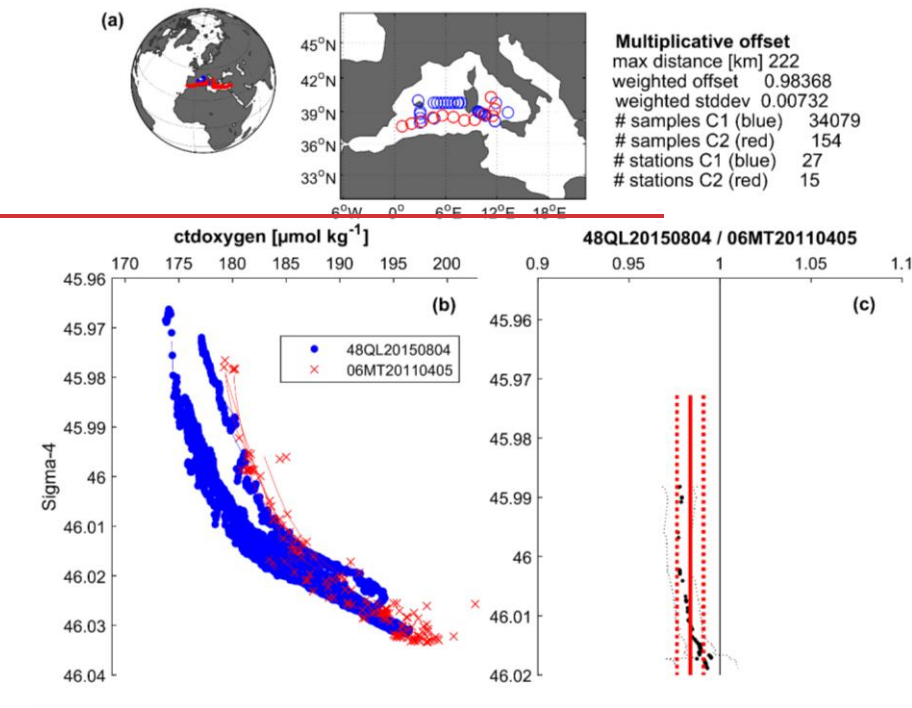
Figure 9 illustrates an example of a crossover and offset between cruise pairs over the entire region, while an overview of some crossovers vs. reference dataset are displayed in Section 4. All calculated offsets for each cruise were examined to determine the presence of any likely biases in the measurements.

The number of stations in the overlapping region (i.e., within the predefined radius) is critical for accurate offset estimation. For instance, as depicted in Figure 8 (a), 30 stations from C1 were compared to 14 stations from C2 to estimate the offset; a limited number of stations can introduce uncertainty into the offset estimate. Additionally, while the number of crossover cruises is significant, the Mediterranean Sea has a limited number of reference cruises available.

Corrections Factor (CF) is estimated from the offset. CF were meticulously reviewed and justified whenever adjustments were deemed necessary (Table 4), at this step, a set of potential correction factor is estimated from the difference offsets. Here, we followed a conservative approach, we are comparing the median regional offsets and choose to apply the correction factor with an absolute low percent of change (deviation from 1). This approach is ensuring low change in the data and improves the internal consistency of the data.

Following adjustments/corrections, the last step involves evaluation the overall internal consistency of the entire dataset CTDO2-WMED using the weighted mean (WM) of the absolute offsets (D) of all crossovers (L) and the standard deviation (σ), following Tanhua et al. (2009) and Belgacem et al. (2020). This assessment quantifies the accuracy of the data product, as supported by previous studies (Hoppema et al., 2009; Sabine et al., 2010; Tanhua et al., 2009). Notably, our evaluation is based on offsets relative to a reference dataset, providing a comprehensive understanding of data consistency.

703 $WM = \frac{\sum_{i=1}^L D(i)/(\sigma(i))^2}{\sum_{i=1}^L 1/(\sigma(i))^2}$



704

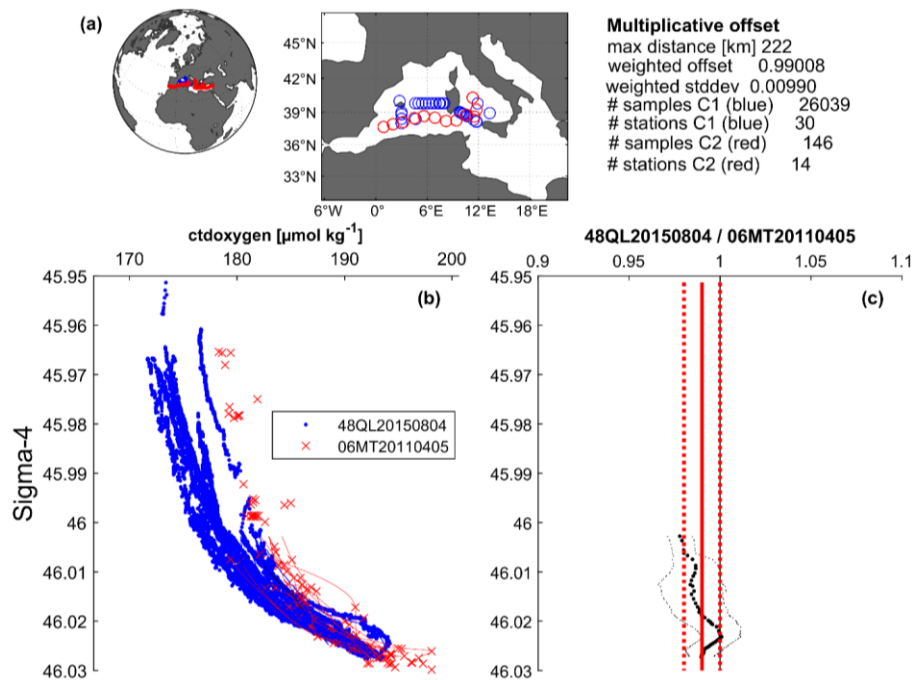


Figure 9. An illustration showcasing the calculated offset for dissolved oxygen between cruise 48QL20150804 and cruise 06MT20110405 (reference cruise). (a) Spatial distribution of CTD stations involved in the crossover analysis, along with statistical information. (b) Vertical profiles of dissolved oxygen observation ($\mu\text{mol}/\text{kg}$) from both cruises that fall within the radius of 2° (800- 2500 dbar). (c) Display of the difference between both cruises (thick dotted black line), standard deviation (thin dotted black lines), the weighted average of the offset (solid red line), and the weighted standard deviation (dotted red line).

Figure 8. An illustration showeasing the calculated offset for dissolved oxygen between cruise 48QL20150804 and cruise 06MT20110405 (reference cruise). (a) Spatial distribution of CTD stations involved in the crossover analysis, along with statistical information. (b) Vertical profiles of dissolved oxygen observation ($\mu\text{mol}/\text{kg}$) from both cruises that fall within the radius of 2° (>1000 dbar). (c) Display of the difference between both cruises (thick dotted black line), standard deviation (thin dotted black lines), the weighted average of the offset (solid red line), and the weighted standard deviation (dotted red line).

4 Results of the secondary QC and recommendations

The outcomes of the crossover analysis are presented in terms of correction factors derived from comparisons with selected reference cruises (Table 2). These corrections, aimed at enhancing measurement consistency, are summarized in Table 4. The analysis assumes that the reference dataset represents the true values. This section details the various crossovers, discusses the offsets, and outlines the derived correction factors. Each crossover was thoroughly evaluated, and corrections were refined as necessary, considering the number of crossovers, regional difference and the stations involved in each comparison.

The offsets and correction factors for each cruise indicated small changes. Few cruises fell outside the predefined accuracy envelope of 2% and therefore required adjustments. Notably, cruises no. 25: 48DP20180918, no. 27:

48DP20221015, and no. 28; 48DP20230324 were excluded from the crossover analysis due to an insufficient number of stations below 800 dbar; however, these cruises remain available in the final dataset.

In total, 265 crossovers were identified (including the entire extent and regional clustering) of the cruises and the regional. The analysis suggested that deep oxygen measurements from specific cruises (no. 2, no.8, no.211 and no.222) necessitated upward adjustment when compared to the reference cruises in the region. Conversely, cruises no. 3, no. 5, and no. 24 exhibited slightly elevated values relative to the respective reference datasets, indicating a need for downward adjustments. Fourteen cruises did not require any corrections, demonstrating consistency with the reference dataset and indicating a high quality of the measurements. A correction is endorsed when the offset is outside the predefined accuracy envelope of $\pm 2\%$.

Table 3 and Figure 10, resume the possible improvements after corrections. In the subsequent text, a thorough discussion about the adjustments (i.e., Correction factor) of the main challenging cruises is provided. The reader is invited to compare the descriptions with the respective plots in Figure 10 and the corresponding crossover summary figures for each cruise.

To validate our findings, we recalculated the offsets using the adjusted data after applying the corrections outlined in Table 4.

Following the application of these adjustments, the offsets were reduced. The suggested cruises now fall within the accepted envelope of 2% indicating an enhanced consistency of the measurements. This improvement is evident in the adjusted data presented in Figure 10(in blue).

To evaluate the consistency, we computed WM using the offsets of the crossover estimated the selected adjusted data, Figure 11. The level of internal consistency of the adjusted CTD oxygen dataset is estimated to 0.998. The adjustments removed potential biases arising from errors related to measurement, calibration, data handling practices, and the lack of adherence to international standards improving the overall consistency.

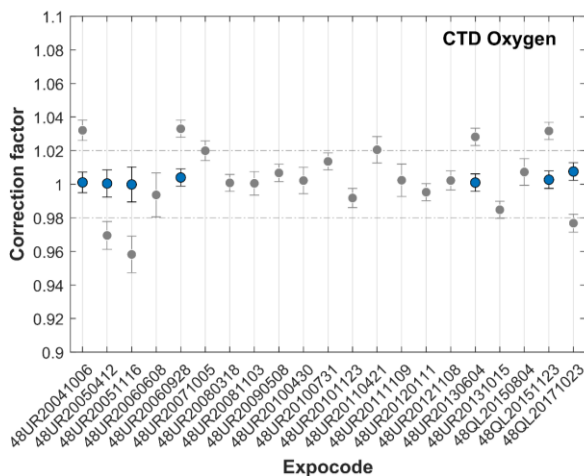


Figure 10. Results of the crossover analysis results for CTD dissolved oxygen, showing the recommended correction before (in grey) and after (in blue) adjustment. Error bars indicate the standard deviation of the absolute weighted offset. A correction means the original CTD Oxygen data must be multiplied by that amount (see Table 4). The dashed line represents the 2% accuracy envelope for an adjustment to be made.

analysis applied to the CNR dissolved oxygen CTD data collected in the WMED are presented in terms of correction factors derived from comparisons with selected reference cruises (GLODAP, CARIMED, MedSHIP). These corrections, aimed at enhancing measurement consistency, are summarized in Table 4. The analysis assumes that the reference dataset represents the true values. This section details the various crossovers, discusses the offsets, and outlines the derived correction factors.

Each crossover was thoroughly evaluated, and corrections were refined as necessary, considering the number of crossovers and the stations involved in each comparison. The offsets and correction factors for each cruise indicated that a significant number of cruises fell outside the predefined accuracy envelope of 1% (as discussed in Section 3.2) and therefore required adjustments. Notably, cruises no. 25, no. 27, and no. 28 were excluded from the crossover analysis due to an insufficient number of stations below 1000 dbar; however, these cruises remain available in the data product.

In total, 73 crossovers were identified. The analysis suggested that deep oxygen measurements from specific cruises (no. 2, no. 8, no. 9, no. 15, no. 17, no. 211, no. 222, and no. 23) necessitated upward adjustment when compared to the reference cruises in the region. Conversely, cruises no. 3, no. 5, no. 21, and no. 24 exhibited slightly elevated values relative to the respective reference datasets, indicating a need for downward adjustments.

Eight cruises (no. 6, no. 10, no. 11/12, no. 13, no. 14, no. 16, no. 18, no. 20, and no. 22) did not require any corrections, demonstrating consistency with the reference dataset and indicating a high quality of the measurements. A correction is endorsed when the offset exceeds the predefined accuracy envelope of $\pm 1\%$. Overall, minor adjustments are proposed, reflecting the overall good quality of the data.

The range of all correction factors was 0.097 (difference between minimum and maximum value), with the most substantial correction factor reaching 1.05, assigned to cruise 48UR20130604 (no. 211). Correction factors varied between 0.95 and 0.975 (for adjustments ≤ 1) and between 1.018 and 1.05 (for adjustments > 1 ; refer to Table 4 and Fig. 9).

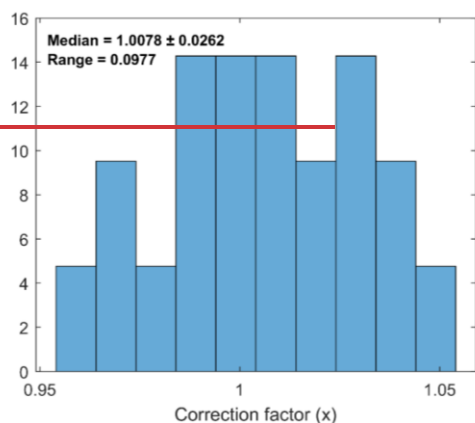


Figure 9. Distribution of multiplicative correction factor.

Table 5, Figure 10, and Figure S1 assesses the possible improvements after corrections. In the subsequent text, a thorough discussion about the adjustments (i.e., Correction factor) of the main challenging cruises is provided. The reader is invited to compare the descriptions with the respective plots in Figure 10 and the corresponding crossover summary figures for each cruise.

Table 3. Summary of the suggested multiplicative adjustments for CTD dissolved oxygen resulting from the 2nd quality control

Cruise ID	EXPOCODE	Recommended correction (x)
2	48UR20041006	1.032
3	48UR20050412	0.97
5	48UR20051116	0.96
6	48UR20060608	-
8	48UR20060928	1.03
9	48UR20071005	-
10	48UR20080318	-
11/12 ^a	48UR20080905/48UR20081103	-
13	48UR20090508	-
14	48UR20100430	-
15	48UR20100731	-
16	48UR20101123	-
17	48UR20110421	-
18	48UR20111109	-
20	48UR20120111	-
21	48UR20121108	-
211	48UR20130604	1.028

22	48UR20131015	—
222	48QL20151123	1.03
23	48QL20150804	—
24	48QL20171023	0.97

^a Cruise #11 and cruise #12 were merged in the 2nd QC.

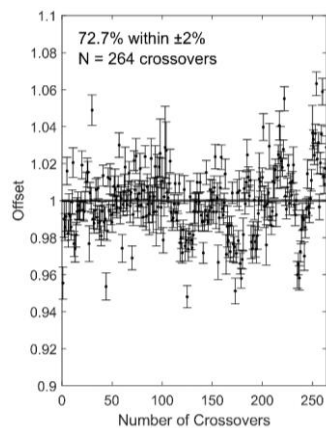


Figure 11. offsets calculated from CTD oxygen crossovers in CTDO2-WMED dataset after applying correction factors. N is number of crossovers.

Table 4. Summary of the suggested multiplicative adjustments for dissolved oxygen (x) resulting from the crossover analysis.

Cruise ID	EXPOCODE	Correction factor (x)
2	48UR20041006	1.0329
3	48UR20050412	0.975
5	48UR20051116	0.9655
6	48UR20060608	—
8	48UR20060928	1.031
9	48UR20071005	1.025
10	48UR20080318	—
11/12 ^a	48UR20080905/48UR20081103	—
13	48UR20090508	—
14	48UR20100430	—
15	48UR20100731	1.034
16	48UR20101123	—
17	48UR20110421	1.022
18	48UR20111109	—
20	48UR20120111	—
21	48UR20121108	0.973
211	48UR20130604	1.02852
22	48UR20131015	—
222	48QL20151123	1.039
23	48QL20150804	1.018
24	48QL20171023	0.970

^aCruise #11 and cruise #12 were merged in the secondary QC.

- Cruise no. 2 (48UR20041006) CTD-O2 adjustments

Formatted: Normal, Left

Formatted: Font color: Text 1

Formatted: Font color: Text 1

Formatted: Font color: Text 1

Formatted: Font color: Text 1

Formatted: Font color: Text 1

Formatted: Font color: Text 1

Formatted: Font color: Text 1

Formatted: Font color: Text 1

Formatted: Font color: Text 1

Formatted: Font color: Text 1

Formatted: Font color: Text 1

Formatted: Font color: Text 1

In section, we provide interpretations and recommendations supporting the proposed adjustments, including discussion of any potential offsets identified, even for cruise where no correction was ultimately applied. Cruises not mentioned here showed consistent CTD oxygen data and required no further review. All applied corrections are summarized in Table 3.

Cruise no. 2 (48UR20041006) has crossovers in three sub-regions: two in the Alboran sea, five and four in the Algerian basin and the Tyrrhenian. Offsets in the three regions demonstrated a consensus regarding a mean offset of 0.96 to 0.96 (Fig. 12).

agree about the increase and data of cruise 48UR20041006 seems to be lower than the reference cruises by 4%. In Figure 3, the mean residual between Winkler and Sensor was higher than 2 $\mu\text{mol/kg}$, which might indicate calibration issue. While this increase may appear excessive, it is important to consider that the regional deep averages obtained from cruise no.2 were the lowest (Fig. 5). Adding to this, the WMED deep layer before 2004, has stable ventilation, it is after 2004 the decline in ventilation has been noted. This may provide a rational for the adjustment. That is to say that cruise 48UR20041006 could not have lower. We are applying in all regions the lowest correction factor that changes in a minimum way the data among the different regions which is an increase of 3.2% that means a correction factor of 1.032.

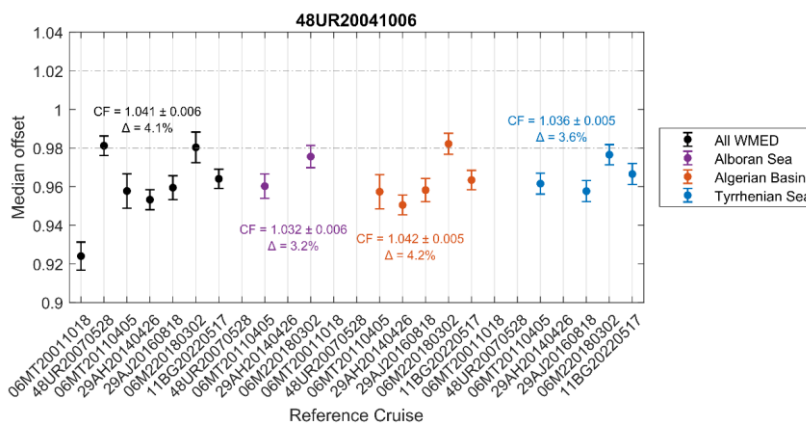


Figure 12. Summary of offsets for all crossovers found for CTD oxygen on cruise no. 2/48UR20041006. The solid red line indicates the weighted mean of the offsets, with its standard deviation in dashed lines; the dashed grey lines denote the predefined accuracy limits for Oxygen measurements; the black dots with error bars illustrate the weighted median offsets in relation to individual reference cruises, along with their corresponding weighted standard deviations in all WMED, the purple is for the Alboran Sea, Orange for the Algerian basin and blue for the Tyrrhenian. The correction factor, standard deviation, and percentage of change of these offsets in each subregion are annotated within the figure. Note that the reference cruises along the x-axis are arranged in chronological order for the different subregions.

Data from cruise **no.3 48UR20050412** was compared to the same reference cruises as cruise no.2. The offset between cruise no.3 and the reference cruises in the Algerian basin with five crossovers and four crossovers in the Tyrrhenian Sea indicates that an adjustment toward a decrease is necessary. As pointed out in section 3.1 cruise no.3 could be of low precision compared to cruises conducted in the same regions.

Based on the agreement between the offsets in both the two subregions (Fig. 13), and even though the crossover with reference 2001 showed good agreement (based on 3 station in 3 different geographic areas), it does not seem robust. So, for this cruise, the offset we are using the overall offset of 1.03 (all WMED), that suggests correction factor of 0.97 which supports a downward adjustment of ~3 %.

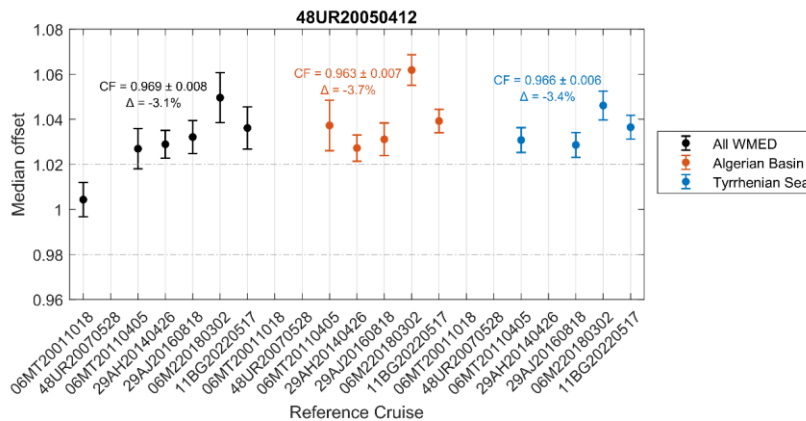


Figure 13. The same as Fig.12 but for cruise no.3 48UR20050412

Cruise no. 5 (48UR20051116) had four crossovers in the Tyrrhenian Sea spanning the years 2011, 2016, 2018 and 2022 (Fig.S3). there is a good agreement in terms of in the precision shown in the weighted standard deviation of 0.01. A median of the weighted offset of 1.042 is found. Based on this, an adjustment toward a decrease of ~4.2% is suggested for cruise no.5. The discrepancy may indicate potential issues with sensor. An adjustment of 0.96 is suggested.

Cruise no. 6 (48UR20060608) has five crossovers in the Algerian basin and four in the Tyrrhenian Sea (Fig. 14). Offsets in the overall basin and in the Algerian basin showed an increased trend of the offset with time. Seven crossovers out of 9 from both subregions were within the 2% envelope.

Here the dynamic between both subregion is clear, low weighted standard deviation of 0.005 in the Tyrrhenian indicate the good precision and good agreement between the four crossovers. In area the variability is less pronounced. While in the Algerian known to be highly variable area, and very much representing the direct effect of the Gulf on Lion, had larger standard deviation of 0.01 persistent in all with references except the 2022 reference.

We refrained from adjusting the data because most of the crossovers did not show consistency between regions and potential trends is observed similar to average vertical profile in Fig.7(c) of the reference cruises in the Algerian and there was good agreement with the references. The majority of the crossover fall within the 2% accuracy. No adjustment is needed.

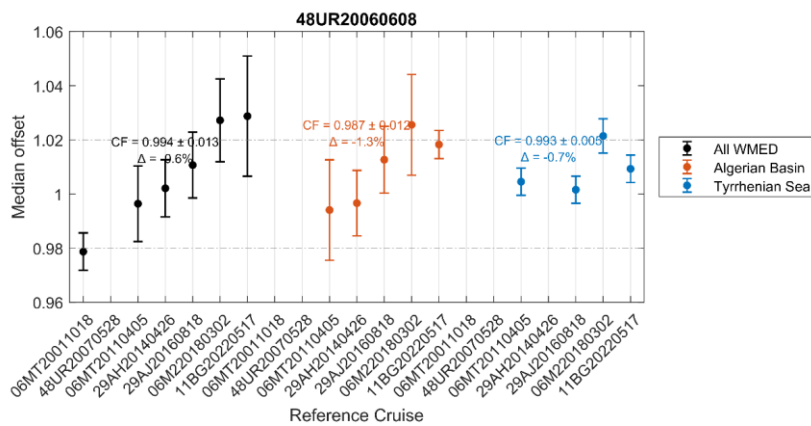


Figure 14. The same as Fig.12 but for Cruise no. 6 (48UR20060608).

Cruise no. 8 (48UR20060928) four crossovers in the Tyrrhenian Sea with reference cruises 06MT20110405, 29AJ20160818, 06M220180302 and 11BG20220517, they all agree about the 0.005 standard deviation and the good quality of the data (Fig. S4). All offsets vary between 0.96 and 0.97 pointing to a correction toward an increase of ~3%. The offsets are outside the 2% envelope. Here we suggest an adjustment of 1.03.

Cruise no. 9 (48UR20071005) has five crossovers in the Algerian basin and four crossovers in the Tyrrhenian Sea. All showing median standard deviation of 0.005 indicative of the good precision of the data. Median weighted offset of 0.97 is recorded in the Tyrrhenian and 0.98 in the Algerian basin. The largest offset was with 06MT20011018, where the offset is about 0.95 (Fig. 15), likely due to the large scatter among the limited number of stations in both sub-regions. Despite, both subregions show a consistent deviation of about the 2% increase, thus suggesting a correction factor of 1.02 that is within the 2% envelope. Therefore, no correction is recommended for this cruise.

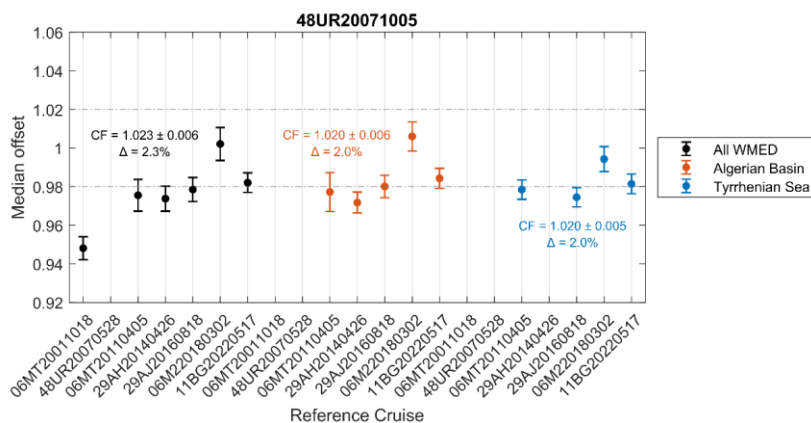


Figure 15. The same as Fig.12 but for Cruise no. 9 (48UR20071005).

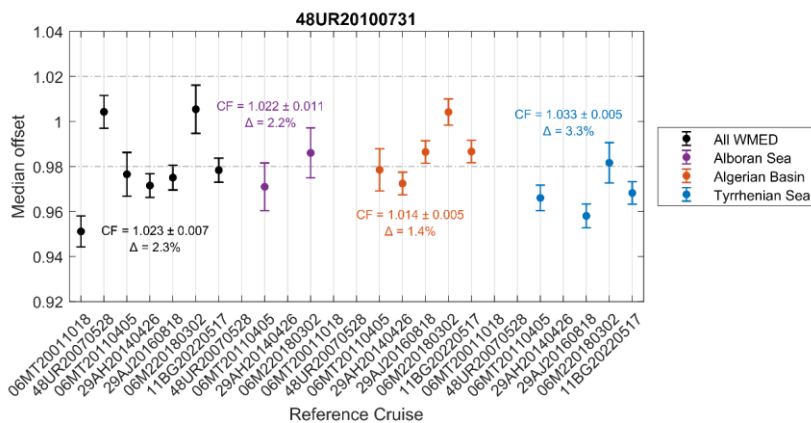


Figure 16. The same as Fig.12 but for Cruise no. 15 (48UR20100731).

Cruise no. 211 (48UR20130604) has an offset of 6% increase in oxygen observed the Algerian basin. A lower offset magnitude is noted in the Tyrrhenian proposing an increase of 2.8%. Both median offsets indicate that oxygen data for this cruise are lower than the references, although data precision appears good. In contrast, cruise **no. 22 (48UR20131015)** from the same year shows smaller offsets magnitude in both regions (Fig.S5), suggesting its oxygen values are higher than the references and might require a small downward adjustment. However, the proposed correction factor 0.98 ± 0.005 for cruise no.22 remain within the 2 % envelope, so no adjustment is applied. For cruise no.211, the differing offset magnitudes between the Algerian and Tyrrhenian (6% vs. 2.8%, respectively, Fig. 17) present a discrepancy; to balance these regional differences while respecting the predefined $\pm 2\%$ envelope, we recommend applying a correction factor of 1.028. this value reflects the smaller offset found in the Tyrrhenian Sea and avoids overcorrecting the data, ensuring consistency.

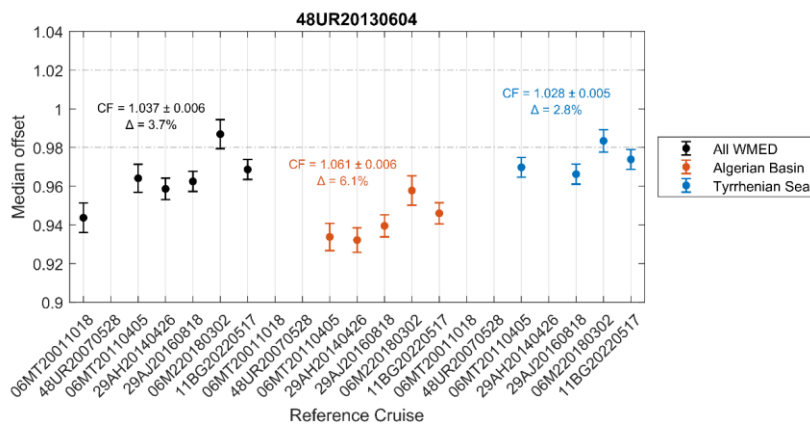


Figure 17. The same as Fig.12 but for Cruise no. 211 (48UR20130604).

Cruise no. 222 (48QL20151123) show a consistent median offset of 0.97 across four crossovers in the Tyrrhenian Sea, spanning multiple years (Fig. S6). The data exhibit good precision, with a weighted standard deviation of 0.005, however, the persistent offset magnitude indicates a systematic underestimation of the oxygen relative to the reference. Deep measurement from this cruise seems to be lower than the reference suggesting a correction of 3% toward an increase, corresponding to a correction factor of 1.03.

Cruise no. 24 (48QL20171023) has four crossovers over the Tyrrhenian Sea (Fig. S7) and shows CTD oxygen values were slightly higher than the reference cruises. The median offset suggests a decrease of approximately 2.3%, indicating a correction factor of 0.97. precision remain high with, weighted standard deviation of 0.005. Additionally, as shown in Figure 3, the means residuals between Winkler and sensor measurements for this cruise was classified as poor, further supporting the need for adjustment. We decided to apply the correction.

x

has crossovers with four references. While this increase may appear excessive, it is important to consider that the regional deep averages obtained from cruise no.2 (Table3) were the lowest. This may provide a rational for the adjustment.

factor that changes in a minimum way the data which that means a correction factor of 1.032. Notably, the crossover with the reference 06MT20011018 indicated that cruise no.2 had lower values, attributed to the limited number of crossover stations available for comparison. The remaining three reference cruises demonstrated a consensus regarding a mean offset of 0.96 (Fig. 10). The offset observed between cruise 48UR20041006 and the reference 06MT20110405 (7 years difference), 29AH20140426 (10 years difference) and 29AJ20160818 (12 years difference) suggest a 4% increase.

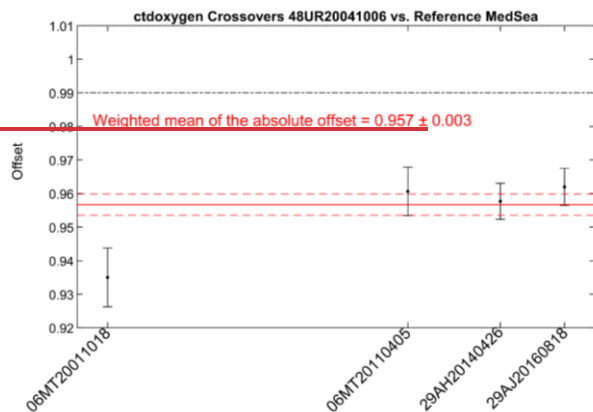


Figure 10. Summary of offsets for all crossovers found for CTD-oxygen on cruise no. 2/48UR20041006. The solid red line indicates the weighted mean of the offsets, with its standard deviation in dashed lines; the dashed grey lines denote the predefined accuracy limits for Oxygen measurements; the black dots with error bars illustrate the weighted mean offsets in relation to individual reference cruises, along with their corresponding weighted standard deviations. The weighted mean and standard deviation of these offsets are annotated within the figure. Note that the reference cruises along the x-axis are arranged in chronological order.

Data from cruise no.3 48UR20050412 was compared to the same reference cruises as cruise no.2. The offset between cruise no.3 and the reference cruises indicates that an adjustment to decrease oxygen is necessary. As pointed out in section 3.1 cruise no.3 exhibited low precision compared to cruises conducted in the same regions. Besides, Figures 10 and 11 illustrate similar behaviors with the reference dataset. For this cruise, the offset the overall offset of 1.03 (all WMED), that suggests correction is 1.025 of 0.97 which supports a downward adjustment of $\sim 3\%$.

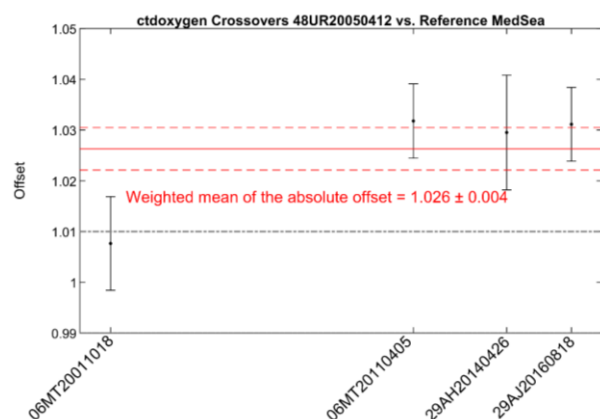


Figure 11. the same as Fig.10 but for no.3 48UR20050412

Formatted: Normal

Formatted: Justified

Formatted: Normal, Justified

Cruise no. 5 (48UR20051116) had two crossovers with the references 06MT20110405 and 29AJ20160818 (Fig.12) in the precision shown in the An offset of 1.045 is computed. Based on this, an adjustment toward a decrease of ~5% is suggested for cruise no.5. The discrepancy may indicate potential issues with Winkler values or sensor calibration. An adjustment of 0.96 is suggested.

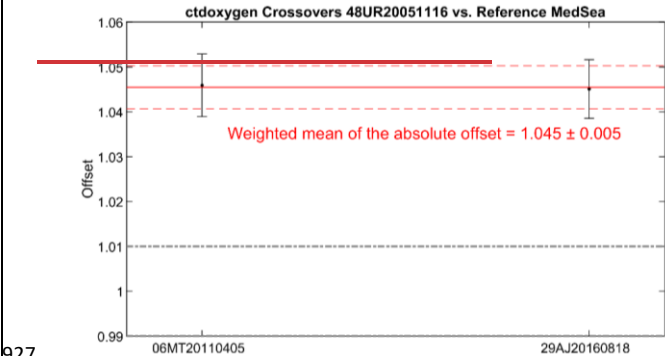


Figure 12. the same as Fig.10 but for no. 5 (48UR20051116)

Formatted: Normal, Justified

Cruise no. 6 (48UR20060608) has five crossovers (Fig. 13). This cruise has few crossover stations with cruise 48UR20070528 which appears to explain the quite large 1.06 offset. The decrease in the measurements is perceived with crossovers 29AH20140426 and 29AJ20160818 which pointed to similar offset of 1.026 which means a downward correction of 3%.

While crossovers with 06MT20110405 and 06MT20011018 do not propose any offset, and cruise no.6 seemed to agree in some parts of the crossing regions;

We refrained from adjusting the data because most of the crossovers did not show consistency and there was good agreement with the references of years 2001 and 2011.

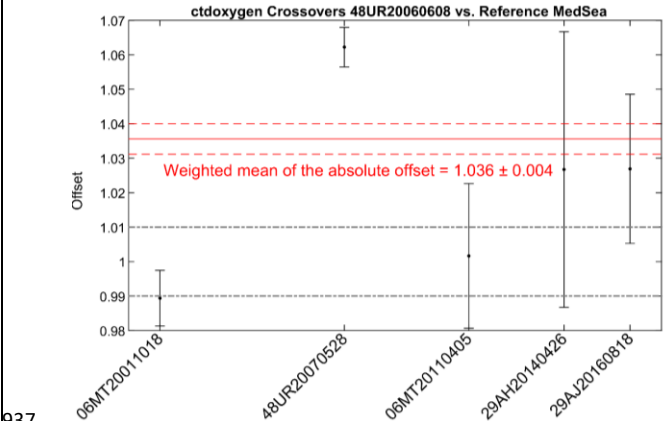
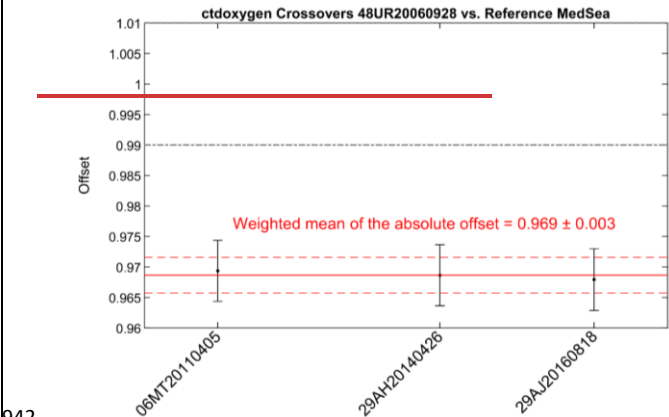


Figure 13. the same as Fig.10 but for Cruise no. 6 (48UR20060608)

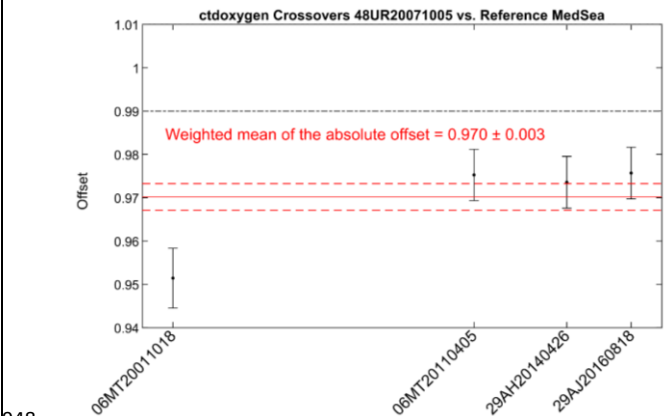
Formatted: Normal, Justified

939 **Cruise no. 8 (48UR20060928)** has three crossovers in the Tyrrhenian Sea with reference cruises 06MT20110405,
940 29AH20140426 and 29AJ20160818 (Fig. 14). All three offsets (0.97) point to the same correction toward an
941 increase of 3%. An adjustment of 1.03 is recommended.



942
943 **Figure 14.** the same as Fig.10 but for **Cruise no. 8 (48UR20060928)**.

944 **Cruise no. 9 (48UR20071005)** has four crossovers. All showing an offset of 0.97 except the crossover with
945 06MT20011018, where the offset is about 0.95 (Fig. 15). This seems to be large because of the large scatter of the
946 ~~few stations in the crossing region. d~~Considering the crossovers with 06MT20110405 29AH20140426 and
947 29AJ20160818, an adjustment of 3% toward an increase is recommended.



948
949 **Figure 15.** the same as Fig.10 but for **Cruise no. 9 (48UR20071005)**

950 **Cruise no. 11 (48UR20080905)** has no crossover points with the selected reference dataset. Since it has a two-
951 month difference from the same year of **cruise no. 12 (48UR20081103)**, both cruises were merged. This 2008
952 cruise has five crossovers. Crossovers with 06MT20011018 show a large offset of 0.97 which means an increase
953 of 3%. Though, crossover with 48UR20070528 shows a large offset of 1.03 suggesting a decrease of 3%. Both

Formatted: Normal, Justified

Formatted: Normal, Justified

crossovers have three crossover points disseminated in different subregions. Their offsets are noticeably higher when compared to the offsets observed in crossovers with the reference cruises 06MT20110405, 29AH20140426 and 29AJ20160818 (Fig.16). However, cruise no.11/12 conducted in 2008, consistently shows no significant offset. Based on this evidence and the inconsistency in the 2001 and 2007 crossovers, we decided for no adjustments

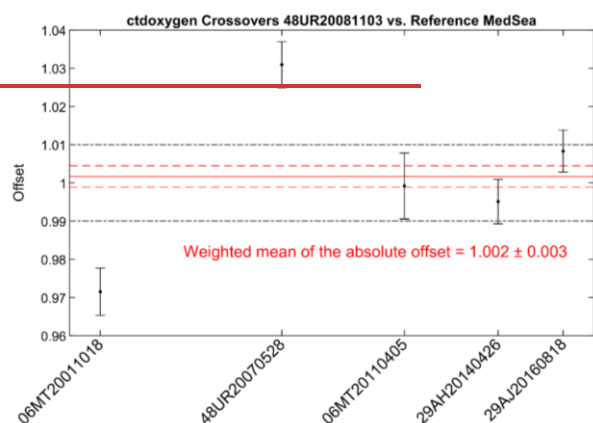


Figure 16. the same as Fig.10 but for Cruise no. 11 and no. 12.

Cruise no. 15 (48UR20100731) has four crossovers. Crossover with 06MT20011018 show very large offset of 0.95 suggesting 5% increase. With few stations in the crossing regions, this crossover is not warrant of reliable adjustment.

Crossovers with 06MT20110405 (one year difference), complies with the singular crossovers with the reference 29AH20140426 (4 years difference) and 29AJ20160818 (six years difference) about an offset of ~0.97 (Fig.17), which gives further evidence for an adjustment of 3% increase.

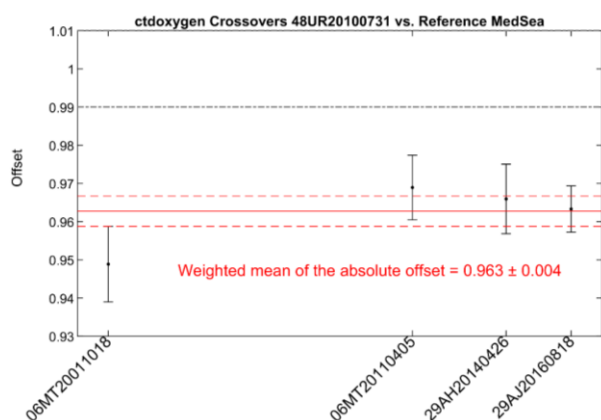


Figure 17. The same as Fig.10 but for Cruise no. 15 (48UR20100731).

Formatted: Normal, Justified

Formatted: Normal, Justified

Cruise no. 17 (48UR20110421) has two crossovers in the Tyrrhenian Sea both agree about an offset of 0.97 (Fig.18). Based on this, an adjustment of 2% toward an increase is suggested. Crossover with same year reference cruise 06MT20110405 gave offset of 0.97. Same offset and adjustments are suggested to cruise no. 8 (48UR20060928) in the same region. This demonstrates additional evidence about the suggested adjustment of cruise no.17, to make it consistent with the neighboring cruises.

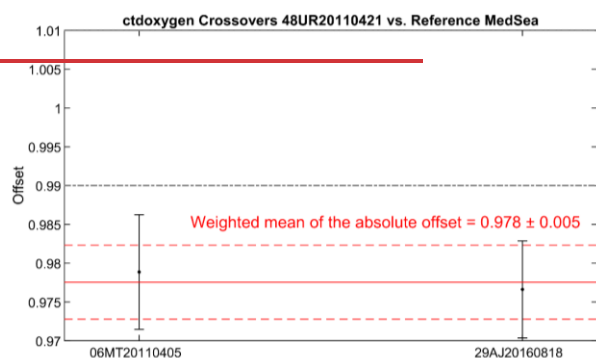


Figure 18. The same as Fig.10 but for Cruise no. 17 (48UR20110421)

Formatted: Normal, Justified

Cruise no. 18 (48UR20111109) has four crossovers. Offsets with the same year reference cruises 06MT20110405 are in good agreement, same with offsets computed with 29AH20140426 (3 years difference) and 29AJ20160818 (5 years difference) that were 0.99 (Fig. 19). Except with crossover with 06MT20011018 (10 years difference) suggestion an offset of 0.97 and an adjustment of 2% increase. Few crossover stations are used to estimate the offset which explains the large offset compared to the other reference. Hence, we have concluded to refrain from making any adjustments.

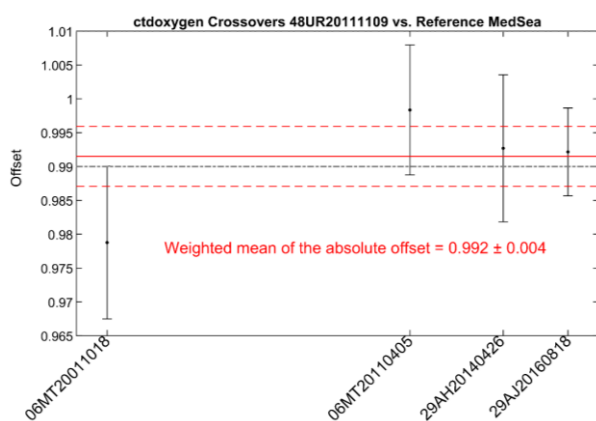


Figure 19. the same as Fig.10 but for Cruise no. 18 (48UR20111109).

Formatted: Normal, Justified

Cruise no. 21 (48UR20121108) has three crossovers with the reference cruises (Fig. 20). In view of crossovers with 06MT20110405 (one-year difference), an offset of 1.026 is found suggesting that the data appear high than the reference and require a downward adjustment of $\sim 3\%$. The adjustment appears justified because the offset with the references 29AH20140426 and 29AJ20160818 suggest similar offset magnitude. Consequently, the adjustment was set to a decrease of 3%.

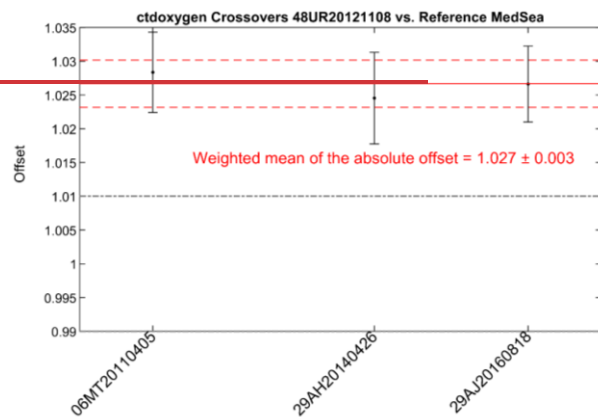


Figure 20. The same as Fig.10 but for Cruise no. 21 (48UR20121108).

Cruise no. 211 (48UR20130604) has an offset of 56% increase in the Algerian basin. A lower extend offset is noted in the tyrrhenian proposing an increase of 2.8%. both median offsets in both region agree about oxygen data in this cruise are lower than the references. The precision seems good of similar magnitude in all crossovers with the four reference cruises 06MT20011018, 06MT20110405, 29AH20140426 and 29AJ20160818 (Fig. 21). Cruise 48UR20130604 seems to be high. Connecting Relating it this to cruise no. 22 (48UR20131015) from the same year, this cruise is showing positive offset in both algerian and tyrrhenian sea indicating that the data are higher than the reference and decrease is needed. looking at the overall crossovers in the WMED, it may indicate a trend. The disagreement in the percentage of change in both region is clear. Besides we choose the lowest percent of change, the correction factor is 1.015 within the 2 % envelope. No adjustment is applied here.

But for cruise 48UR20130604 an upward adjustment of 2.8% is suggested, that means a correction factor of 1.028 is applied.

in good accord with the same reference cruises in the same crossing areas and did not show any offset, providing additional evidence. We think that an adjustment of 5% toward an increase is justified to bring the data within the acceptable range.

Formatted: Normal, Justified

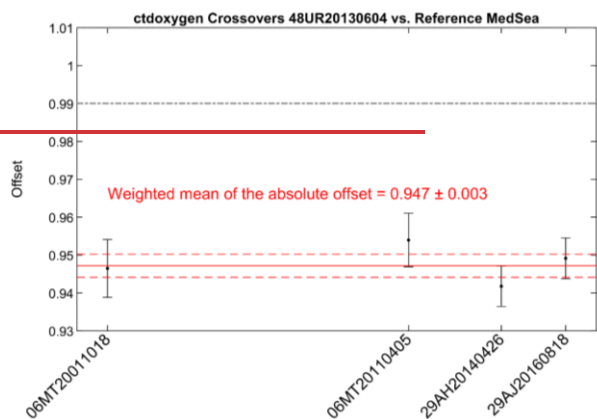


Figure 21. The same as Fig.10 but for Cruise no. 211 (48UR20130604).

Cruise no. 222 (48QL20151123) has a consistent offset of 0.96 ⁹⁷ with all three crossovers spanning different years—with cruises 06MT20110405 (four year difference), 29AH20140426 (one year difference) and 29AJ20160818 (1 year difference), and 11BG20220517 in the tyrrhenain sea(Fig. 22). the precision of data is good with a weighted standard deviation of 0.005, but the accuracy seems to low. deep measurement from this cruise seems to be lower than the reference suggesting a correction of 42% toward an increase, which means a correction factor of 1.03.:

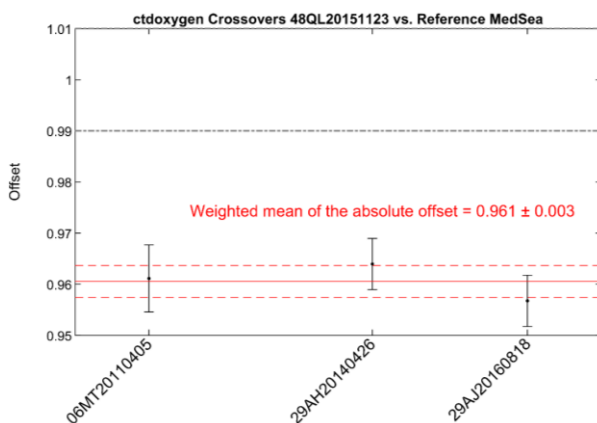


Figure 22. The same as Fig.10 but for Cruise no. 222 (48QL20151123).

Similar increase is apparent in Cruise no. 23 (48QL20150804) happened in the same year 2015. Three crossovers with the references 06MT20110405, 29AH20140426 and 29AJ20160818 agree about a ~2% increase based on a

Formatted: Normal, Justified

Formatted: Normal, Justified

mean offset of 0.98 (Fig. 23), whereas crossover with the reference cruise 06MT20011018 (14 years difference) propose an offset of 0.96, accordingly 4% increase, which is very high and not enough justified. We therefore suggest a correction following the three references.

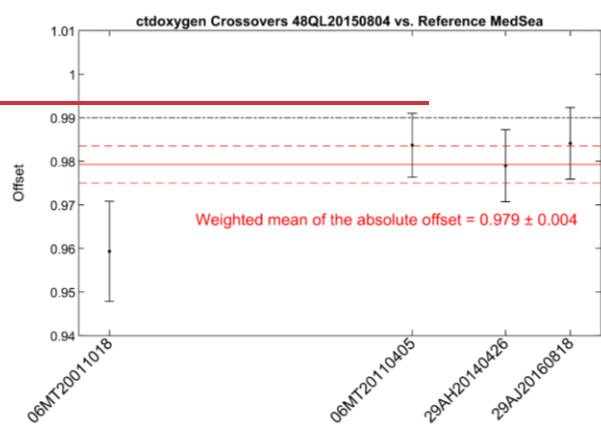
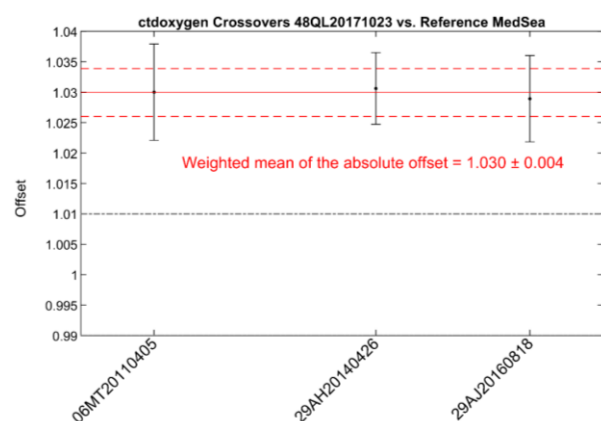


Figure 23. The same as Fig.10 but for Cruise no. 23 (48QL20150804).

And finally, cCruise no. 24 (48QL20171023) has three crossovers (Fig. 24) over the Tyrrhenian sea. its leasurments were slightly higher than the reference cruises, suggesting a correction factor of 0.97, a decrease of 2.3% with the reference 06MT20110405 (six years difference), 29AH20140426 (three years) and 29AJ20160818 (one year difference). The weighted standard deviation was about 0.005 across all crossover indicative of the good precision of the data. looking at figure XX where the means residual between wonkler and sensor for this cruise was classifies as poor. A constant offset of 1.029 is assessed indicating that cruise no.24 is higher than the reference. The offset appears to be persistent in all these years and is suggestive of an adjustment of 3% toward a decrease, that should be appropriate. We decided to follow the suggestion apply the correction.



Formatted: Normal, Justified

Formatted: Justified

1034
1035
1036
1037
1038
1039
1040
1041
1042
1043
1044
1045
1046
1047

1048
1049
1050
1051
1052
1053

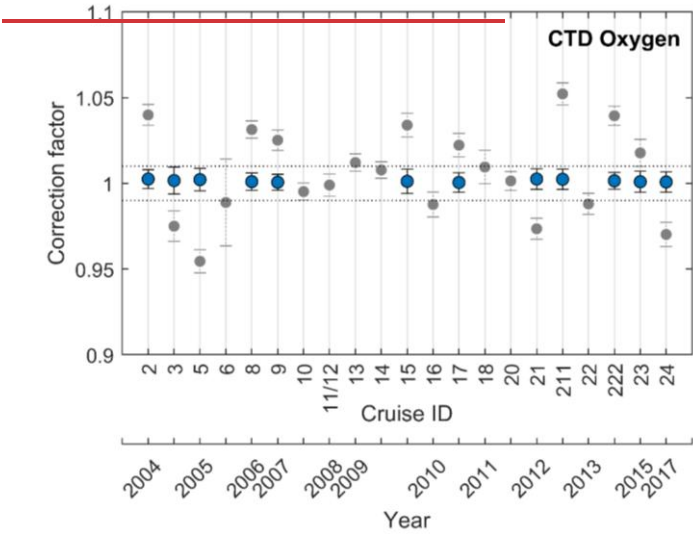
Figure 24. The same as Fig.10 but for Cruise no. 24 (48QL20171023).

To validate our findings, we recalculated the offsets using the adjusted data after applying the corrections outlined in Table 4.

Following the application of these adjustments, the offsets were reduced. The suggested cruises now fall within the accepted envelope of 1% indicating an enhanced consistency of the measurements. This improvement is evident in the adjusted data presented in Figure 25 (in blue) and table 4.

To evaluate the consistency, we computed WM of the absolute offsets. The consistency of the adjusted oxygen dataset experienced a slight enhancement, increasing from 0.991 to 0.998%. This corresponds to an improvement in the internal consistency of the dataset by 0.7%. The minor improvement in consistency, coupled with the reduced range, underscores the high quality of the initial dataset and efficacy of the quality assurance procedures implemented during each cruise.

The adjustments removed potential biases arising from errors related to measurement, calibration, data handling practices, and the lack of adherence to international standards improving the overall consistency.



Formatted: Justified

Figure 25. Results of the crossover analysis results for CTD dissolved oxygen, showing the correction before (in grey) and after (in blue) adjustment. Error bars indicate the standard deviation of the absolute weighted offset. A correction means the original CTD Oxygen data must be multiplied by that amount (see Table 4). The dashed line represents the 1% accuracy envelope for an adjustment to be made.

Formatted: Normal

1054 Table 5. Results from the Secondary QC: improvements of the weighted mean of absolute offset per cruise
 1055 for both unadjusted and adjusted data. “n” represents the number of crossovers per cruise. Values in bold
 1056 (>1) signify instances where the measurements from the tested cruises are lower than the reference data.

Formatted: Justified, Line spacing: 1,5 lines

Cruise ID	EXPOCODE	n	CTD-Oxygen (%)		Crossover regions
			Unadjusted	Adjusted	
2	48UR20041006	4	0.96 ±0.006	0.99±0.005	Tyrrhenian-sea Algerian-basin Alboran-sea
3	48UR20050412	4	1.025±0.008	0.99±0.007	Tyrrhenian-sea Sicily-Sardinia-Channel Algerian-basin Alboran-sea
5	48UR20051116	2	1.045±0.006	0.99±0.006	Tyrrhenian-Sea Sicily-Sardinia-Channel
6	48UR20060608	5	1.01±0.02	NA	Ligurian-Sea Tyrrhenian-Sea Algerian-basin Sardinia-Balearic-sea
8	48UR20060928	3	0.96 ±0.005	0.99±0.005	Ligurian-Sea Tyrrhenian-Sea Algerian-basin Sardinia-Balearic-sea
9	48UR20071005	4	0.97 ±0.005	0.99±0.004	Tyrrhenian-Sea Algerian-basin Sardinia-Balearic-sea
10	48UR20080318	2	1.004±0.005	NA	Tyrrhenian-Sea
11/12	48UR20080905/48UR20081103	5	1.001±0.006	NA	Tyrrhenian-Sea Sicily-Sardinia-Channel Algerian-Basin Alboran-Sea
13	48UR20090508	3	0.989 ±0.005	NA	Tyrrhenian-Sea Sicily-Sardinia-channel
14	48UR20100430	4	0.99 ±0.004	NA	Tyrrhenian-Sea Algerian-basin Sardinia-Balearic-sea Sicily-Sardinia-channel
15	48UR20100731	4	0.96 ±0.006	0.999±0.007	Tyrrhenian-Sea Sicily-Sardinia-channel Algerian-basin Alboran-Sea
16	48UR20101123	2	1.012±0.07	NA	Tyrrhenian-Sea
17	48UR20110421	2	0.97 ±0.006	0.999±0.005	Tyrrhenian-Sea Sicily-Sardinia-channel
18	48UR20111109	4	0.99 ±0.009	NA	Tyrrhenian-Sea Algerian-basin Sardinia-Balearic-sea
20	48UR20120111	4	0.99 ±0.005	NA	Tyrrhenian-Sea Sicily-Sardinia-channel Algerian-basin Sardinia-Balearic-sea
21	48UR20121108	3	1.026±0.006	0.99±0.006	Tyrrhenian-Sea Sardinia-Balearic-sea Sardinia-channel
211	48UR20130604	4	0.950 ±0.006	0.997±0.005	Tyrrhenian-Sea Sicily-Sardinia-channel Algerian-basin Sardinia-Balearic-sea
22	48UR20131015	4	1.012±0.006	NA	Tyrrhenian-Sea Sicily-Sardinia-channel Algerian-basin Sardinia-Balearic-sea
222	48QL20151123	3	0.96 ±0.005	0.998±0.004	Tyrrhenian-Sea Sicily-Sardinia-channel

23	48QL20150804	4	0.98±0.007	0.999±0.006	Ligurian-Sea Tyrrhenian-Sea Algerian-basin Sardinia-Balearic-sea
24	48QL20171023	3	1.029±0.007	0.99±0.005	Tyrrhenian-Sea Sicily-Sardinia-channel

5 Summary and conclusions

6 This study aimed to evaluate and enhance the consistency and accuracy of CTD oxygen measurements in the
7 WMED by implementing the 2nd QC procedure based on crossover analysis. Recognizing the limitations of
8 applying a uniform 1% accuracy envelope; originally developed for the Atlantic datasets; we identified a more
9 regionally appropriate threshold of $\pm 2\%$ for the deep Mediterranean layers, particularly within 800-2000 db
10 range. This adjustment better reflects the natural variability and ventilation dynamics specific to the region.

11 As part of the 2nd QC of the CTDO₂-WMED dataset, a total of 265 crossover comparison were conducted,
12 both spatially and regionally, using a set of high-quality reference cruises. The methodology presented here
13 provides a robust framework for future quality control efforts in regions with similarly complex hydrographic
14 conditions. While the majority of cruises fell within the revised $\pm 2\%$ envelope, a few showed systematic
15 offsets that warranted correction. Adjustments were applied conservatively, only when deviations exceeded
16 the defined threshold and considering the lowest percentage of change; and are recommended for seven
17 cruises. Although the quality of these cruises is considerate moderate, they remain valuable for long-term
18 trend analyses. Rather than being flagged, they are included in the final product. These adjustments led to
19 measurable improvements in data consistency, increasing the internal agreement across cruises, as evidenced
20 by the weighted mean of 0.998. Although a few cruises lacked sufficient deep profiles to perform crossover
21 analysis, their data are retained in the final dataset. Importantly, the dataset aligns with FAIR data principles,
22 and openly accessible.

23 Despite limitations in temporal coverage and the finite number of reference cruises, this updated dataset
24 significantly enhances our understanding of long-term dissolved oxygen variability in the WMED. It
25 complements and extends earlier efforts in the region (Schneider et al., 2014; Coppola and al. (2017); Moriarty
26 et al., 2017; Macías et al., 2018b; Mavropoulou et al., 2020; Li & Tanhua (2020); Cossarini et al.,
27 2021; Friedland et al., 2021; Ulses and al. (2021), and Fourier et al. (2022).

28 Dissolved oxygen is a robust tracer for assessing both physical and biogeochemical changes, carrying the
29 imprint of water mass since their last ventilation. As global warming increases ocean stratification (Oschlies
30 et al., 2008), vertical mixing and thus oxygen renewal is expected to decline, contributing to long-term
31 deoxygenation. This trend is further amplified by increasing ocean heat content and acidification in surface
32 layer (Yao et al., 2016; Reale et al., 2021).

33 Given the scarcity of high-resolution oxygen observations in space and time, recent advances using model
34 simulations, machine learning, and autonomous platforms such as BGC-Argo floats and gliders are crucial.
35 The CTDO₂-WMED dataset, in combination with these emerging sources, provides a valuable foundation for
36 assessing changes in the oxygen budget of the Mediterranean Sea. it supports ongoing efforts to understand
37 the region's response to climate -driven oceanographic changes and to improve future projections.

1091 This study's main objective was to enhance data quality, assurance, and accessibility within the context of FAIR
1092 data principles. Acknowledging the limitations of the reference datasets is essential; although considered high
1093 quality, they are not infallible and may not fully cover the entire temporal range of interest. Regardless, our quality
1094 control efforts have yielded positive results, as demonstrated throughout this study.

1095 The majority of the CTD oxygen data now falls within the predefined acceptance range of 1%, indicating a
1096 consistent and accurate dataset. This aligns with established standards seen in widely used datasets, such as
1097 CARINA and GLODAP (Hoppema et al., 2009; Tanhua et al., 2009). Furthermore, the adjustments made to
1098 address systematic biases between reference datasets and the CNR cruises have significantly improved the internal
1099 consistency of Oxygen measurements.

1100 Despite the inherent challenges in assessing changes in oxygen levels due to the scarcity of measurements, the
1101 recent oxygen data contribute substantially to our understanding of oxygen variability in the region.

1102 The CNR-O2WMED dataset serves as a valuable regional resource, providing quality-controlled measurements
1103 that facilitate accurate trend quantification and estimation of changes, thereby making it an essential tool for future
1104 studies with acceptable temporal and spatial coverage, and the potential extension of the analysis to the Eastern
1105 Mediterranean Sea. The utility of this dataset extends to its assimilation into ocean models and the verification of
1106 regional models, offering critical insights in the oxygen cycle.

1107 While the current dataset does not incorporate data from various sources to avoid potential inconsistencies,
1108 ensuring the reliability of the CNR-O2WMED data remains a priority before any future integrations. The dataset's
1109 utility will be maximized when used in conjunction with other data sources, such as BGC Argo and glider data,
1110 allowing for more comprehensive analysis of the oxygen dynamics in the WMED.

1111 Future studies should focus on synergizing regional datasets to enhance our understanding of ongoing changes in
1112 Biogeochemical cycles. This collaborative approach will ultimately contribute to global efforts to monitor and
1113 mitigate the impacts of ocean deoxygenation, fostering a deeper understanding of biogeochemical processes and
1114 their implications for marine ecosystems.

1115 Future studies should focus on synergizing regional datasets to enhance our understanding of the ongoing changes,
1116 ultimately contribution to global efforts to monitor and mitigate the impact of ocean deoxygenation.

1117 **6.11 Data availability**

1118 The CNR_O2WMEDv1 (Belgacem et al., 2024 [in review], see temporary link below) dataset is available at
1119 PANGAEA (submitted on 21/08/2024, DOI in preparation). It consists of two parts: the first an aggregation of the
1120 cruises prior correction which has undergone both calibration and 1st quality check. The second is the adjusted data
1121 product using the recommended corrections from the secondary quality control. The dataset is complementary to
1122 the data product CNR-DIN-WMED available <https://doi.org/10.1594/PANGAEA.904172>. No special software is
1123 required to access the data. the data from the reference cruises are not included in the final product. Table 6
1124 summarizes the list of parameters included.

1125 The CNR_O2WMEDv1 (Belgacem et al., 2024 [in review], see temporary link below) dataset is available at
1126 PANGAEA (submitted on 21/08/2024, DOI in preparation). It consists of two parts; the first an aggregation of the

Formatted: Font: (Default) +Headings CS (Times New Roman), 10 pt, Complex Script Font: +Headings CS (Times New Roman), 10 pt

Formatted: Normal, No bullets or numbering

Formatted: Font: (Default) +Headings CS (Times New Roman), 10 pt, Complex Script Font: +Headings CS (Times New Roman), 10 pt

1127 cruises prior correction which has undergone both calibration and 1st quality check. The second is the adjusted data
 1128 product using the recommended corrections from the secondary quality control. The dataset is complementary to
 1129 the data product CNR-DIN-WMED available <https://doi.org/10.1594/PANGAEA.904172>. No special software is
 1130 required to access the data.

1131 Temporary link to CNR_O2WMED_ODV format:

1132 [https://cnrsc-](https://cnrsc-my.sharepoint.com/:f:/g/personal/malekbelgacem_cnr_it/EkIgo958UMIBmJ8SGwNB4HwBBX-FzDa8N9C3vHeS4Vd4Q?e=Wt8pII)
 1133 [my.sharepoint.com/:f:/g/personal/malekbelgacem_cnr_it/EkIgo958UMIBmJ8SGwNB4HwBBX-](https://cnrsc-my.sharepoint.com/:f:/g/personal/malekbelgacem_cnr_it/EkIgo958UMIBmJ8SGwNB4HwBBX-FzDa8N9C3vHeS4Vd4Q?e=Wt8pII)
 1134 [FzDa8N9C3vHeS4Vd4Q?e=Wt8pII](https://cnrsc-my.sharepoint.com/:f:/g/personal/malekbelgacem_cnr_it/EkIgo958UMIBmJ8SGwNB4HwBBX-FzDa8N9C3vHeS4Vd4Q?e=Wt8pII)

1135 Table 6 summarizes the list of parameters included.

1136 **Table 46. Summary of data product parameters and units.**

Variable	Data Product file parameter name	Data product WOCE flag name	Units
Expedition/cruise code	EXPOCODE		
Cruise ID	CRUISE		
Station number	STNNBR		
Year	YEAR		
Month	MONTH		
Day	DAY		
Latitude	LATITUDE		decimal degree
Longitude	LONGITUDE		decimal degree
Pressure	CTDPRS		decibar
Temperature	CTDTMP		°C
Salinity	CTDSAL	CTDSAL_FLAG_W	
Oxygen	CTDOXY	CTDOXY_FLAG_W	μmol kg ⁻¹

1137

1138

1139 Authors contributions

1140 MaB ran the analysis and wrote the manuscript. KS contributed to writing the manuscript. MA, SKL contributed
 1141 to the analysis. JC contributed to specific parts of the manuscript. MiB and SS coordinated the technical aspects
 1142 of most of the cruises. CC and TC assisted some of the chemical analysis and contributed to write the analytical
 1143 method.

1144 Competing interest

1145 The authors declare that they have no conflict of interest.

1146 Acknowledgements

1147 [M. Belgacem was supported by the EuroGO-SHIP project funded by European Union under grant agreement no.](#)
 1148 [101094690. The data have been collected in the framework of several national and European projects, e.g.](#)
 1149 [KM3NeT, EU GA no. 011937; SESAME, EU GA no. GOCE-036949; PERSEUS, EU GA no. 287600; OCEAN-](#)
 1150 [CERTAIN, EU GA no. 603773; COMMON SENSE, EU GA no. 228344; EUROFLEETS, EU GA no. 228344;](#)
 1151 [EUROFLEETS2, EU GA no. 312762; JERICO, EU GA no. 262584; and the Italian PRIN 2007 program](#)
 1152 [“Tyrrhenian Seamounts ecosystems” and the Italian RITMARE flagship project, both funded by the Italian](#)

Field Code Changed

1153 [Ministry of Education, University and Research. We acknowledge PRIN-CLOSER “CLimate forcing On Adriatic](#)
1154 [SEa deoxygenation: A multi-archive Reconstruction of Sapropel S1 \(CLOSER\)” project funded by the Italian](#)
1155 [Ministry of Education and European Union NextGenerationEU. The authors are deeply indebted to all](#)
1156 [investigators and analysts who contributed to data collection at sea during so many years as well as to the PIs of](#)
1157 [the cruises \(Stefano Cozzi, Gabriella Cerrati, Stefano Aliani, Mario Astraldi, Maurizio Azzaro, Alberto Ribotti,](#)
1158 [Massimiliano Dibitto, Gian Pietro Gasparini, Annalisa Griffo, Jeff Haun, Loïc Jullion, Gina La Spada, Elena](#)
1159 [Mannini, Angelo Perilli and Chiara Santinelli\), the captains, and the crews for allowing the collection of this](#)
1160 [enormous dataset; without them, this work would not have been possible.](#)

1161 The data have been collected in the framework of several national and European projects, e.g. KM3Net, EU GA
1162 no. 011937; SESAME, EU GA no. GOCE-036949; PERSEUS, EU GA no. 287600; OCEAN-CERTAIN, EU GA
1163 no. 603773; COMMON SENSE, EU GA no. 228344; EUROFLEETS, EU GA no. 228344; EUROFLEETS2, EU
1164 GA no. 312762; JERICO, EU GA no. 262584; and the Italian PRIN 2007 program “Tyrrhenian Seamounts
1165 ecosystems” and the Italian RITMARE flagship project, both funded by the Italian Ministry of Education,
1166 University and Research. The authors thank the Horizon Europe —IA REDRESS project for the funding.

1167 The authors are deeply indebted to all investigators and analysts who contributed to data collection at sea during
1168 so many years as well as to the PIs of the cruises (Stefano Cozzi, Gabriella Cerrati, Stefano Aliani, Mario Astraldi,
1169 Maurizio Azzaro, Alberto Ribotti, Massimiliano Dibitto, Gian Pietro Gasparini, Annalisa Griffo, Jeff Haun, Loïc
1170 Jullion, Gina La Spada, Elena Mannini, Angelo Perilli and Chiara Santinelli), the captains, and the crews for
1171 allowing the collection of this enormous dataset; without them, this work would not have been possible.

1172 Reference

1173 [Álvarez, M., Sanleón-Bartolomé, H., Tanhua, T., Mintrop, L., Luchetta, A., Cantoni, C., Schroeder, K., and](#)
1174 [Civitares, G.: The CO₂ system in the Mediterranean Sea: a basin wide perspective, Ocean Sci., 10, 69–92,](#)
1175 <https://doi.org/10.5194/os-10-69-2014>, 2014.

1176 [Álvarez, M., Catalá, T. S., Civitares, G., Coppola, L., Hassoun, A. E. R., Ibello, V., Lazzari, P., Lefevre, D.,](#)
1177 [Marcias, D., Santinelli, C., and Ulses, C: Chapter 11–Mediterranean Sea general biogeochemistry, Editor \(s\):](#)
1178 [Katrin Schroeder, Jacopo Chiggiato, Oceanography of the Mediterranean Sea, https://doi.org/10.1016/B978-0-12-](#)
1179 [823692-5.00004-2](https://doi.org/10.1016/B978-0-12-823692-5.00004-2), 2022.

1180 [Belgacem, M., Chiggiato, J., Borghini, M., Pavoni, B., Cerrati, G., Acri, F., Cozzi, S., Ribotti, A., Álvarez, M.,](#)
1181 [Lauvset, S. K., and Schroeder, K.: Quality controlled dataset of dissolved inorganic nutrients in the western](#)
1182 [Mediterranean Sea \(2004–2017\) from R/V oceanographic cruises, PANGAEA \[data set\],](#)
1183 <https://doi.org/10.1594/PANGAEA.904172>, 2019.

1184 [Belgacem, M., Chiggiato, J., Borghini, M., Pavoni, B., Cerrati, G., Acri, F., Cozzi, S., Ribotti, A., Álvarez, M.,](#)
1185 [Lauvset, S. K., and Schroeder, K.: Dissolved inorganic nutrients in the western Mediterranean Sea \(2004–2017\),](#)
1186 [Earth Syst. Sci. Data, 12, 1985–2011, https://doi.org/10.5194/essd-12-1985-2020](#), 2020.

1187 [Belgacem, M., Schroeder, K., Lauvset, S. K., Álvarez, M., Chiggiato, J., Borghini, M., Cantoni, C., Ciuffardi, T.,](#)
1188 [Sparnocchia, S.: O2WMED: Quality controlled dataset of dissolved oxygen in the western Mediterranean Sea](#)
1189 [\(2004–2023\) from R/V oceanographic cruises \[dataset\], PANGAEA, in review: temporary link: https://cnrsc-](#)
1190 [my.sharepoint.com/:f/g/personal/malekbelgacem_cnr_it/EkIgo958UMIBmJ8SGwNB4HwBBX-](https://cnrsc-my.sharepoint.com/:f/g/personal/malekbelgacem_cnr_it/EkIgo958UMIBmJ8SGwNB4HwBBX-FzDa8N19C3vHeS4Vd4Q?e=Wt8p1I)
1191 [FzDa8N19C3vHeS4Vd4Q?e=Wt8p1I](https://cnrsc-my.sharepoint.com/:f/g/personal/malekbelgacem_cnr_it/EkIgo958UMIBmJ8SGwNB4HwBBX-FzDa8N19C3vHeS4Vd4Q?e=Wt8p1I), 2024.

1192 [Coppola, L., Prieur, L., Taupier-Letage, I., Estournel, C., Testor, P., Lefevre, D., Belamari, S., & Taillandier, V.:](#)
1193 [Observation of oxygen ventilation into deep waters through targeted deployment of multiple Argo-O₂ floats in the](#)

1194 north-western Mediterranean Sea in 2013, *J. Geophys. Res.-Oceans*, 122, 6325–6341,
1195 <https://doi.org/10.1002/2016JC012594>, 2017.

1196 Coppola, L., Legendre, L., Lefevre, D., Prieur, L., Taillandier, V., & Riquier, E. D. (2018). Seasonal and inter-
1197 annual variations of dissolved oxygen in the northwestern Mediterranean Sea (DYFAMED site). *Progress in*
1198 *Oceanography*, 162, 187–201, <https://doi.org/10.1016/j.pocean.2018.03.001>, 2018.

1199 Cossarini, G., Feudale, L., Teruzzi, A., Bolzon, G., Coidessa, G., Solidoro, C., Di Biagio, V., Amadio, C., Lazzari,
1200 P., Brosich, A., and Salon, S.: High-resolution reanalysis of the Mediterranean Sea biogeochemistry (1999–2019),
1201 *Front. Mar. Sci.*, 8, 741486, <https://doi.org/10.3389/fmars.2021.741486>, 2021.

1202 Fichaut, M., Garcia, M. J., Giorgetti, A., Iona, A., Kuznetsov, A., Rixen, M., and Medar Group:
1203 MEDAR/MEDATLAS 2002: A Mediterranean and Black Sea database for operational oceanography, Elsevier
1204 *Oceanography Series*, 69, 645–648, [https://doi.org/10.1016/S0422-9894\(03\)80107-1](https://doi.org/10.1016/S0422-9894(03)80107-1), 2003.

1205 Fourrier, M., Coppola, L., Lebrato, M., Testor, P., Bosse, A., D'Ortenzio, F., Taillandier, V., de Madron, X. D.,
1206 Mortier, L., Prieur, L., and Gatti, J.: Impact of intermittent convection in the northwestern Mediterranean Sea on
1207 oxygen content, nutrients, and the carbonate system, *J. Geophys. Res.-Oceans*, 127, e2022JC018615,
1208 <https://doi.org/10.1029/2022JC018615>, 2022.

1209 Friedland, R., Macias, D., Cossarini, G., Daewel, U., Estournel, C., Garcia-Gorriz, E., Grizzetti, B., Grégoire, M.,
1210 Gustafson, B., Kalaroni, S., Kerimoglu, O., Lazzari, P., Lenhart, H., Lessin, G., Maljutenko, I., Miladinova, S.,
1211 Müller-Karulis, B., Neumann, T., Parn, O., Pätsch, J., Piroddi, C., Raudsepp, U., Schrum, C., Stegert, C., Stips,
1212 A., Tsiaras, K., Ulses, C., and Vandenbulcke, L.: Effects of nutrient management scenarios on marine
1213 eutrophication indicators: a pan-European, multi-model assessment in support of the Marine Strategy Framework
1214 Directive, *Front. Mar. Sci.*, 8, 596126, <https://doi.org/10.3389/fmars.2021.596126>, 2021.

1215 Garcia and Gordon (1992) "Oxygen solubility in seawater: Better fitting equations", *Limnology & Oceanography*,
1216 vol 37(6), p1307-1312.

1217 Grasshoff, K., Ehrhardt, M., and Kremling, K.: *Methods of Seawater Analysis*, 2nd Edition, Verlag Chemie
1218 Weinheim, New York, 419 p., 1983.

1219 Grasshoff, K., Kremling, K., and Ehrhardt, M.: *Methods of seawater analysis* (3rd edn.), Weinheim Press, WILEY-
1220 VCH, 203–273, 1999.

1221 Grégoire, M., Oschlies, A., Canfield, D., Castro, C., Ciglenečki, I., Croot, P., Salin, K., Schneider, B., Serret, P.,
1222 Slomp, C.P., Tesi, T., Yücel, M. (2023). Ocean Oxygen: the role of the Ocean in the oxygen we breathe and the
1223 threat of deoxygenation. Rodriguez Perez, A., Kellett, P., Alexander, B., Muñiz Piniella, Á., Van Elslander, J.,
1224 Heymans, J. J., [Eds.] Future Science Brief No. 10 of the European Marine Board, Ostend, Belgium. ISSN: 2593-
1225 5232. ISBN: 9789464206180. DOI: 10.5281/zenodo.7941157, 2023.

1226 Guy, S.-V., Kress, N., Silverman, J., Gertner, Y., Ozer, T., Biton, E., Lazar, A., Gertman, I., Rahav, E., and Herut,
1227 B.: Post-eastern Mediterranean Transient Oxygen Decline in the Deep Waters of the Southeast Mediterranean Sea
1228 Supports Weakening of Ventilation Rates, *Front. Mar. Sci.*, 7, <https://doi.org/10.3389/FMARS.2020.598686>,
1229 2021.

1230 Hainbucher, D., Rubino, A., Cardin, V., Tanhua, T., Schroeder, K., and Bensi, M.: Hydrographic situation during
1231 cruise M84/3 and P414 (spring 2011) in the Mediterranean Sea, *Ocean Sci.*, 10, 669–682,
1232 <https://doi.org/10.5194/os-10-669-2014>, 2014.

1233 Helen, R., Powley, Krom, M. D., Van Cappellen, P.: Circulation and oxygen cycling in the Mediterranean Sea:
1234 Sensitivity to future climate change, *J. Geophys. Res.*, <https://doi.org/10.1002/2016JC012224>, 2016.

1235 Hoppema, M., Velo, A., van Heuven, S., Tanhua, T., Key, R. M., Lin, X., Bakker, D. C. E., Perez, F. F., Ríos, A.,
1236 F., Lo Monaco, C., Sabine, C. L., Álvarez, M., and Bellerby, R. G. J.: Consistency of cruise data of the CARINA
1237 database in the Atlantic sector of the Southern Ocean, *Earth Syst. Sci. Data*, 1, 63–75, <https://doi.org/10.5194/essd-1-63-2009>, 2009.

1239 Janzen, C., Murphy, D., and Larson, N.: Getting more mileage out of dissolved oxygen sensors in long-term
1240 moored applications, *OCEANS 2007, IEEE*, doi: 10.1109/OCEANS.2007.4449398, 2007.

1241 Johnson, G. C., Robbins, P. E., and Hufford, G. E.: Systematic adjustments of hydrographic sections for internal
1242 consistency, *J. Atmos. Ocean. Tech.*, 18, 1234–1244, [https://doi.org/10.1175/1520-0426\(2001\)018<1234:SAOHSF>2.0.CO;2](https://doi.org/10.1175/1520-0426(2001)018<1234:SAOHSF>2.0.CO;2), 2001.

1244 Jullion, L.: TAIPro2016: A Tyrrhenian Sea & Alger-Provençal component of the MedSHIP Programme, *RV*
1245 *Angeles Alvariño*, 18/08/16 – 29/08/16, Palermo (Italy) – Barcelona (Spain), Bremerhaven, EUROFLEETS2
1246 Cruise Summary Report, <https://epic.awi.de/id/eprint/49725/>, 2016.

1247 Keeling, R. F., Körtzinger, A., and Gruber, N.: Ocean deoxygenation in a warming world, *Annu. Rev. Mar. Sci.*,
1248 2, 199–229, doi: 10.1146/annurev.marine.010908.163855, 2010.

1249 Langdon, C.: Determination of Dissolved Oxygen in Seawater by Winkler Titration using Amperometric
1250 Technique, In: Hood, E.M., Sabine, C.L., Sloyan, B.M. (Eds.), *The GO-SHIP Repeat Hydrography Manual: A*
1251 *Collection of Expert Reports and Guidelines, Version 1, IOCCP Report Number 14, ICPO Publication Series*
1252 *Number 134*, 18pp., <https://doi.org/10.25607/OBP-1350>, 2010.

1253 Lauvset, S. K., and Tanhua, T.: A toolbox for secondary quality control on ocean chemistry and hydrographic data,
1254 *Limnol. Oceanogr. Methods*, 13, 601–608, <https://doi.org/10.1002/lom3.10050>, 2015.

1255 Li P and Tanhua T (2020) Recent Changes in Deep Ventilation of the Mediterranean Sea; Evidence From Long-
1256 Term Transient Tracer Observations. *Front. Mar. Sci.* 7:594. doi: 10.3389/fmars.2020.00594

1257 Liu G., Yu,X., Zhang,J., Wang,X., Xu,N., Ali,S.: Reconstruction of the three-dimensional dissolved oxygen and
1258 its spatio-temporal variations in the Mediterranean Sea using machine learning, *Journal of Environmental*
1259 *Sciences*,2025,ISSN 1001-0742,<https://doi.org/10.1016/j.jes.2025.01.010>.

1260 Manca, B., Burca, M., Giorgetti, A., Coatanoan, C., Garcia, M. J., and Iona, A. Physical and biochemical averaged
1261 vertical profiles in the Mediterranean regions: an important tool to trace the climatology of water masses and to
1262 validate incoming data from operational oceanography, *J. Mar. Syst.*, 48, 83–116,
1263 <https://doi.org/10.1016/j.jmarsys.2003.11.025>, 2004.

1264 Macias, D., Garcia-Gorriz, E., and Stips, A.: Deep winter convection and phytoplankton dynamics in the NW
1265 Mediterranean Sea under present climate and future (horizon 2030) scenarios, *Sci. Rep.*, 8, 6626,
1266 <https://doi.org/10.1038/s41598-018-24978-5>, 2018.

1267 Margirier, F., Testor, P., Heslop, E., Mallil, K., Bosse, A., Houpert, L., Mortier, L., Bouin, M.-N., Coppola, L.,
1268 D’Ortenzio, F., Durrieu de Madron, X., Murre, B., Prieur, L., Raimbault, P., and Taillandier, V.: Abrupt warming
1269 and salinification of intermediate waters interplays with decline of deep convection in the Northwestern
1270 Mediterranean Sea, *Sci. Rep.*, 10, 20923, <https://doi.org/10.1038/s41598-020-77961-9>, 2020.

1271 Martínez, J., Leonelli, F. E., García-Ladona, E., Garrabou, J., Kersting, D. K., Bensoussan, N., and Pisano, A.:
1272 Evolution of marine heatwaves in warming seas: the Mediterranean Sea case study, *Front. Mar. Sci.*, 10, 1193164,
1273 <https://doi.org/10.3389/fmars.2023.1193164>, 2023.

1274 Marullo, S., De Toma, V., di Sarra, A., Iacono, R., Landolfi, A., Leonelli, F., Napolitano, E., Meloni, D., Organelli,
1275 E., Pisano, A., Santoleri, R., and Sferlazzo, D.: Has the frequency of Mediterranean Marine Heatwaves really
1276 increased in the last decades? , *EGU General Assembly 2023, Vienna, Austria*, 23–28 Apr 2023, EGU23-4429,
1277 <https://doi.org/10.5194/egusphere-egu23-4429> , 2023.

1278 Mavropoulou, A.-M., Vervatis, V., and Sofianos, S.: Dissolved oxygen variability in the Mediterranean Sea, *J.*
1279 *Mar. Syst.*, 208, 103348, <https://doi.org/10.1016/j.jmarsys.2020.103348> ,2020.

1280 Mavropoulou, A.-M.: Mediterranean Sea: Dissolved Oxygen, Temperature and Salinity Annual Variability and
1281 Monthly Climatology for the period 1960-2011, <https://doi.org/10.5281/zenodo.3878076> , 2020.

1282 Middleton, L., Wu, W., Johnston, T. M. S., Tarry, D. R., Farrar, J. T., Poulain, P.-M., Özgökmen, T. M.,
1283 Shcherbina, A. Y., Pascual, A., McNeill, C. L., Belgacem, M., Berta, M., Abbott, K., Worden, A. Z., Wittmers,
1284 F., Kinsella, A., Centurioni, L. R., Hormann, V., Cutolo, E., Tintoré, J., Ruiz, S., Casas, B., Cheslack, H.,
1285 CALYPSO Collaboration, D'Asaro, E. A., and Mahadevan, A.: Ocean cyclone splitting ventilates the upper ocean,
1286 *Sci. Adv.*, accepted, 2025.

1287 Moriarty, J. M., Harris, C. K., Fennel, K., Friedrichs, M. A. M., Xu, K., and Rabouille, C.: The roles of
1288 resuspension, diffusion and biogeochemical processes on oxygen dynamics offshore of the Rhône River, France:
1289 a numerical modeling study, *Biogeosciences*, 14, 1919–1946, <https://doi.org/10.5194/bg-14-1919-2017>, 2017.

1290 Olsen, A., Key, R. M., van Heuven, S., Lauvset, S. K., Velo, A., Lin, X., Schirnack, C., Kozyr, A., Tanhua, T.,
1291 Hoppema, M., Jutterström, S., Steinfeldt, R., Jeansson, E., Ishii, M., Pérez, F. F., and Suzuki, T.: The Global Ocean
1292 Data Analysis Project version 2 (GLODAPv2) – an internally consistent data product for the world ocean, *Earth*
1293 *Syst. Sci. Data*, 8, 297–323, <https://doi.org/10.5194/essd-8-297-2016> , 2016.

1294 Olsen, A., Lange, N., Key, R. M., Tanhua, T., Bittig, H. C., Kozyr, A., Álvarez, M., Azetsu-Scott, K., Becker, S.,
1295 Brown, P. J., Carter, B. R., Cotrim da Cunha, L., Feely, R. A., van Heuven, S., Hoppema, M., Ishii, M., Jeansson,
1296 E., Jutterström, S., Landa, C. S., Lauvset, S. K., Michaelis, P., Murata, A., Pérez, F. F., Pfeil, B., Schirnack, C.,
1297 Steinfeldt, R., Suzuki, T., Tilbrook, B., Velo, A., Wanninkhof, R., and Woosley, R. J.: An updated version of the
1298 global interior ocean biogeochemical data product, GLODAPv2.2020, *Earth Syst. Sci. Data*, 12, 3653–3678,
1299 <https://doi.org/10.5194/essd-12-3653-2020> , 2020.

1300 Owens, W. B., and R. C. Millard Jr., 1985: A new algorithm for CTD oxygen calibration. *J. Physical*
1301 *Oceanography*, 15, 621–631.

1302 Pastor, F., and Khodayar, S.: Marine heat waves: Characterizing a major climate impact in the Mediterranean.
1303 EGU General Assembly 2023, Vienna, Austria, 24–28 Apr 2023, EGU23-13058,
1304 <https://doi.org/10.5194/egusphere-egu23-13058>, 2023.

1305 Reale, M., Cossarini, G., Lazzari, P., Lovato, T., Bolzon, G., Masina, S., Solidoro, C., and Salon, S.: Acidification,
1306 deoxygenation, and nutrient and biomass declines in a warming Mediterranean Sea, *Biogeosciences*, 19, 4035–
1307 4065, <https://doi.org/10.5194/bg-19-4035-2022>, 2022.

1308 Ribotti, A., Sorgente, R., Pessini, F., Cucco, A., Quattrocchi, G., and Borghini, M.: Twenty-one years of
1309 hydrological data acquisition in the Mediterranean Sea: quality, availability, and research, *Earth Syst. Sci. Data*,
1310 14, 4187–4199, <https://doi.org/10.5194/essd-14-4187-2022> , 2022.

1311 Schroeder, K., Tanhua, T., Bryden, H., Alvarez, M., Chiggiato, J., and Aracri, S.: Mediterranean Sea Ship-based
1312 Hydrographic Investigations Program (Med-SHIP), *Oceanography*, 28, 12–15,
1313 <https://doi.org/10.5670/oceanog.2015.71> , 2015.

1314 Schneider, A., Tanhua, T., Roether, W., and Steinfeldt, R.: Changes in ventilation of the Mediterranean Sea during
1315 the past 25 year, *Ocean Sci.*, 10, 1–16, <https://doi.org/10.5194/os-10-1-2014>, 2014.

1316 Schroeder, K., Kovačević, V., Civitarese, G., Velaoras, D., Álvarez, M., Tanhua, T., Jullio, L., Coppola, L., Bensi,
1317 M., Ursella, L., Santinelli, C., Giani, M., Chiggiato, J., Aly-Eldeen, M., Assimakopoulou, G., Bachi, G., Bogner,
1318 B., Borghini, M., Cardin, V., Cornec, M., Giannakourou, A., Giannoudi, L., Gogou, A., Golbol, M., Or Hazan, O.,
1319 Karthäuser, C., Kralj, M., Krasakopoulou, E., Matić, F., Mihanović, H., Muslim, S., Papadopoulos, V.P., Parinos,
1320 C., Paulitschke, A., Pavlidou, A., Pitta, E., Protopapa, M., Rahav, E., Raveh, O., Renieris, P., Reyes-Suarez, N.,
1321 C., Rousselaki, E., Silverman, J., Souvermezoglou, E., Urbini, L., Zer, C., and Zervoudaki, S.: Seawater physics
1322 and chemistry along the Med-SHIP transects in the Mediterranean Sea in 2016, *Sci. Data*, 11, 52,
1323 <https://doi.org/10.1038/s41597-023-02835-3>, 2024.

1324 Schroeder, K.: TAIPro2022 CRUISE REPORT R/V BELGICA Cruise n. 2022/12 (Version 1), Zenodo,
1325 <https://doi.org/10.5281/zenodo.6918731> , 2022.

1326 Tanhua, T., Brown, P. J., and Key, R. M.: CARINA: nutrient data in the Atlantic Ocean, *Earth Syst. Sci. Data*, 1,
1327 7–24, <https://doi.org/10.5194/essd-1-7-2009>, 2009.

1328 Tanhua, T.: Matlab Toolbox to Perform Secondary Quality Control (2nd QC) on Hydrographic Data, ORNL
1329 CDIAC-158, Carbon Dioxide Inf. Anal. Center, Oak Ridge Natl. Lab., U.S. Dep. Energy, Oak Ridge, Tennessee,
1330 158, <https://doi.org/10.1002/lom3.10050>, 2010.

1331 Tanhua, T.: Hydrochemistry of water samples during MedSHIP cruise Talpro, PANGAEA,
1332 <https://doi.org/10.1594/PANGAEA.902293>, 2019a.

1333 Tanhua, T.: Physical oceanography during MedSHIP cruise Talpro [dataset], PANGAEA,
1334 <https://doi.org/10.1594/PANGAEA.902330>, 2019b.

1335 Testor, P., Bosse, A., Houpert, L., Margirier, F., Mortier, L., Legoff, H., Dausse, D., Labaste, M., Bouin, M.-N.,
1336 Coppola, L., Koenig, Z., Damien, P., et al.: Multiscale observations of deep convection in the northwestern
1337 Mediterranean Sea during winter 2012–2013 using multiple platforms, *J. Geophys. Res.-Oceans*, 122, 1745–1776,
1338 <https://doi.org/10.1002/2016JC012671>, 2017.

1339 Uchida, H., Johnson, G. C. and McTaggart, G. C.: CTD Oxygen Sensor Calibration Procedures. In: *The GO-SHIP*
1340 *Repeat Hydrography Manual: A Collection of Expert Reports and Guidelines. Version 1*, (eds Hood, E.M., C.L.
1341 Sabine, and B.M. Sloyan), 17pp. (IOCCP Report Number 14; ICPO Publication Series Number 134),
1342 <https://doi.org/10.25607/OBP-1344>, 2010.

1343 Ulses, C., D'Ortenzio, F., Coppola, L., Estournel, C., Testor, P., Marsaleix, P., Prieur, L., Taillandier, V., Dumas,
1344 F., Severin, T., and Conan, P.: Oxygen budget of the north-western Mediterranean deep-convection region,
1345 *Biogeosciences*, 18, 937–960, <https://doi.org/10.5194/bg-18-937-2021>, 2021.

1346 Yao, M., Marcou, O., Goyet, C., Guglielmi, V., Touratier, F., and Savy, J.-P.: Time variability of the north-western
1347 Mediterranean Sea pH over 1995–2011, *Mar. Environ. Res.*, 116, 51–60,
1348 <https://doi.org/10.1016/j.marenvres.2016.02.016>, 2016.

1349 Belgacem, M., Chiggiato, J., Borghini, M., Pavoni, B., Cerrati, G., Aeri, F., Cozzi, S., Ribotti, A., Álvarez, M.,
1350 Lauvset, S. K., and Schroeder, K.: Quality controlled dataset of dissolved inorganic nutrients in the western
1351 Mediterranean Sea (2004–2017) from R/V oceanographic cruises, PANGAEA [data set],
1352 <https://doi.org/10.1594/PANGAEA.904172>, 2019.

1353 Belgacem, M., Chiggiato, J., Borghini, M., Pavoni, B., Cerrati, G., Aeri, F., Cozzi, S., Ribotti, A., Álvarez, M.,
1354 Lauvset, S. K., and Schroeder, K.: Dissolved inorganic nutrients in the western Mediterranean Sea (2004–2017),
1355 *Earth Syst. Sci. Data*, 12, 1985–2011, <https://doi.org/10.5194/essd-12-1985-2020>, 2020.

1356 Belgacem, M., Schroeder, K., Lauvset, S. K., Álvarez, M., Chiggiato, J., Borghini, M., Cantoni, C., Ciuffardi, T.,
1357 Sparnocchia, S.: O2WMED: Quality controlled dataset of dissolved oxygen in the western Mediterranean Sea
1358 (2004–2023) from R/V oceanographic cruises [dataset], PANGAEA, in review: temporary link: [https://cnrsc-](https://cnrsc-my.sharepoint.com/:f/g/personal/malekbelgacem_cnr_it/EkIgo958UMIBmJ8SGwNB4HwBBX-FzDa8NI9C3vHeS4Vd4Q?e=Wt8pH)
1359 [my.sharepoint.com/:f/g/personal/malekbelgacem_cnr_it/EkIgo958UMIBmJ8SGwNB4HwBBX-](https://cnrsc-my.sharepoint.com/:f/g/personal/malekbelgacem_cnr_it/EkIgo958UMIBmJ8SGwNB4HwBBX-FzDa8NI9C3vHeS4Vd4Q?e=Wt8pH)
1360 [FzDa8NI9C3vHeS4Vd4Q?e=Wt8pH](https://cnrsc-my.sharepoint.com/:f/g/personal/malekbelgacem_cnr_it/EkIgo958UMIBmJ8SGwNB4HwBBX-FzDa8NI9C3vHeS4Vd4Q?e=Wt8pH), 2024.

1361 Coppola, L., Legendre, L., Lefevre, D., Prieur, L., Taillandier, V., & Riquier, E. D. (2018). Seasonal and inter-
1362 annual variations of dissolved oxygen in the northwestern Mediterranean Sea (DYFAMED site). *Progress in*
1363 *Oceanography*, 162, 187–201, <https://doi.org/10.1016/j.pocean.2018.03.001>, 2018.

1364 Fichaut, M., Garcia, M. J., Giorgetti, A., Iona, A., Kuznetsov, A., Rixen, M., and Medar Group:
1365 MEDAR/MEDATLAS 2002: A Mediterranean and Black Sea database for operational oceanography, Elsevier
1366 *Oceanography Series*, 69, 645–648, [https://doi.org/10.1016/S0422-9894\(03\)80107-1](https://doi.org/10.1016/S0422-9894(03)80107-1), 2003.

1367 Grasshoff, K., Ehrhardt, M., and Kremling, K.: *Methods of Seawater Analysis*, 2nd Edition, Verlag Chemie
1368 Weinheim, New York, 419 p., 1983.

Field Code Changed

Field Code Changed

Field Code Changed

Field Code Changed

1369 Grasshoff, K., Kremling, K., and Ehrhardt, M.: Methods of seawater analysis (3rd edn.), Weinheim Press, WILEY-
1370 VCH, 203–273, 1999.

1371 Grégoire, M., Osehlies, A., Canfield, D., Castro, C., Ciglenečki, I., Croot, P., Salin, K., Schneider, B., Serret, P.,
1372 Slomp, C.P., Tesi, T., Yücel, M. (2023). Ocean Oxygen: the role of the Ocean in the oxygen we breathe and the
1373 threat of deoxygenation. Rodriguez Perez, A., Kellett, P., Alexander, B., Muñoz Piniella, Á., Van Elslander, J.,
1374 Heymans, J. J., [Eds.] Future Science Brief No. 10 of the European Marine Board, Ostend, Belgium. ISSN: 2593-
1375 5232. ISBN: 9789464206180. DOI: 10.5281/zenodo.7941157, 2023.

1376 Guy, S., V., Kress, N., Silverman, J., Gertner, Y., Ozer, T., Biton, E., Lazar, A., Gertman, I., Rahav, E., and Herut,
1377 B.: Post-eastern Mediterranean Transient Oxygen Decline in the Deep Waters of the Southeast Mediterranean Sea
1378 Supports Weakening of Ventilation Rates, *Front. Mar. Sci.*, 7, <https://doi.org/10.3389/FMARS.2020.598686>,
1379 2021.

1380 Hainbucher, D., Rubino, A., Cardin, V., Tanhua, T., Schroeder, K., and Bensi, M.: Hydrographic situation during
1381 cruise M84/3 and P414 (spring 2011) in the Mediterranean Sea, *Ocean Sci.*, 10, 669–682,
1382 <https://doi.org/10.5194/os-10-669-2014>, 2014.

1383 Helen, R., Powley, Krom, M. D., Van Cappellen, P.: Circulation and oxygen cycling in the Mediterranean Sea:
1384 Sensitivity to future climate change, *J. Geophys. Res.*, <https://doi.org/10.1002/2016JC012224>, 2016.

1385 Hoppema, M., Velo, A., van Heuven, S., Tanhua, T., Key, R. M., Lin, X., Bakker, D. C. E., Perez, F. F., Ríos, A.
1386 F., Lo Monaco, C., Sabine, C. L., Álvarez, M., and Bellerby, R. G. J.: Consistency of cruise data of the CARINA
1387 database in the Atlantic sector of the Southern Ocean, *Earth Syst. Sci. Data*, 1, 63–75, <https://doi.org/10.5194/essd-1-63-2009>, 2009.

1388 Janzen, C., Murphy, D., and Larson, N.: Getting more mileage out of dissolved oxygen sensors in long-term
1389 moored applications, *OCEANS 2007, IEEE*, doi: 10.1109/OCEANS.2007.4449398, 2007.

1390 Johnson, G. C., Robbins, P. E., and Hufford, G. E.: Systematic adjustments of hydrographic sections for internal
1391 consistency, *J. Atmos. Ocean. Tech.*, 18, 1234–1244, [https://doi.org/10.1175/1520-0426\(2001\)018<1234:SAOHSF>2.0.CO;2](https://doi.org/10.1175/1520-0426(2001)018<1234:SAOHSF>2.0.CO;2), 2001.

1392 Jullion, L.: TAIPro2016: A Tyrrhenian Sea & Alger-Provençal component of the MedSHIP Programme, RV
1393 Angeles Alvariño, 18/08/16–29/08/16, Palermo (Italy)–Barcelona (Spain), Bremerhaven, EUROFLEETS2
1394 Cruise Summary Report, <https://epic.awi.de/id/eprint/49725/>, 2016.

1395 Keeling, R. F., Körtzinger, A., and Gruber, N.: Ocean deoxygenation in a warming world, *Annu. Rev. Mar. Sci.*,
1396 2, 199–229, doi: 10.1146/annurev.marine.010908.163855, 2010.

1397 Langdon, C.: Determination of Dissolved Oxygen in Seawater by Winkler Titration using Amperometric
1398 Technique, In: Hood, E.M., Sabine, C.L., Sloyan, B.M. (Eds.), *The GO-SHIP Repeat Hydrography Manual: A
1399 Collection of Expert Reports and Guidelines, Version 1*, IOCCP Report Number 14, ICPO Publication Series
1400 Number 134, 18pp., <https://doi.org/10.25607/OBP-1350>, 2010.

1401 Lauvset, S. K., and Tanhua, T.: A toolbox for secondary quality control on ocean chemistry and hydrographic data,
1402 *Limnol. Oceanogr. Methods*, 13, 601–608, <https://doi.org/10.1002/lom3.10050>, 2015.

1403 Laurent, C., Louis, L., Dominique, L., Louis, M. P., Vincent, T., Emilie, D., and Riquier, D.: Seasonal and inter-
1404 annual variations of dissolved oxygen in the northwestern Mediterranean Sea (DYFAMED site), *Prog. Oceanogr.*,
1405 162, 187–201, <https://doi.org/10.1016/j.pocean.2018.03.001>, 2018.

Field Code Changed

Field Code Changed

Field Code Changed

Field Code Changed

Field Code Changed

Field Code Changed

Field Code Changed

Field Code Changed

Field Code Changed

Manca, B., Burca, M., Giorgetti, A., Coatanoan, C., Garcia, M. J., and Iona, A.: Physical and biochemical-averaged vertical profiles in the Mediterranean regions: an important tool to trace the climatology of water masses and to validate incoming data from operational oceanography, *J. Mar. Syst.*, 48, 83–116, <https://doi.org/10.1016/j.jmarsys.2003.11.025>, 2004.

Álvarez, M., Catalá, T. S., Civitarese, G., Coppola, L., Hassoun, A. E. R., Ibelló, V., Lazzari, P., Lefevre, D., Marcias, D., Santinelli, C., and Ulses, C.: Chapter 11 Mediterranean Sea general biogeochemistry, Editor (s): Katrin Schroeder, Jacopo Chiggiato, *Oceanography of the Mediterranean Sea*, <https://doi.org/10.1016/B978-0-12-823692-5.00004-2>, 2022.

Martínez, J., Leonelli, F. E., García-Ladona, E., Garrabou, J., Kersting, D. K., Bensoussan, N., and Pisano, A.: Evolution of marine heatwaves in warming seas: the Mediterranean Sea case study, *Front. Mar. Sci.*, 10, 1193164, <https://doi.org/10.3389/fmars.2023.1193164>, 2023.

Marullo, S., De Toma, V., di Sarra, A., Iacono, R., Landolfi, A., Leonelli, F., Napolitano, E., Meloni, D., Organelli, E., Pisano, A., Santoleri, R., and Sferlazzo, D.: Has the frequency of Mediterranean Marine Heatwaves really increased in the last decades? , *EGU General Assembly 2023*, Vienna, Austria, 23–28 Apr 2023, EGU23-4429, <https://doi.org/10.5194/egusphere-egu23-4429>, 2023.

Mavropoulou, A. M., Vervatis, V., and Sofianos, S.: Dissolved oxygen variability in the Mediterranean Sea, *J. Mar. Syst.*, 208, 103348, <https://doi.org/10.1016/j.jmarsys.2020.103348>, 2020.

Mavropoulou, A. M.: Mediterranean Sea: Dissolved Oxygen, Temperature and Salinity Annual Variability and Monthly Climatology for the period 1960–2011, <https://doi.org/10.5281/zenodo.3878076>, 2020.

Olsen, A., Key, R. M., van Heuven, S., Lauvset, S. K., Velo, A., Lin, X., Schirnack, C., Kozyr, A., Tanhua, T., Hoppema, M., Jutterström, S., Steinfeldt, R., Jeansson, E., Ishii, M., Pérez, F. F., and Suzuki, T.: The Global Ocean Data Analysis Project version 2 (GLODAPv2)—an internally consistent data product for the world ocean, *Earth Syst. Sci. Data*, 8, 297–323, <https://doi.org/10.5194/essd-8-297-2016>, 2016.

Olsen, A., Lange, N., Key, R. M., Tanhua, T., Bittig, H. C., Kozyr, A., Álvarez, M., Azetsu-Scott, K., Becker, S., Brown, P. J., Carter, B. R., Cotrim da Cunha, L., Feely, R. A., van Heuven, S., Hoppema, M., Ishii, M., Jeansson, E., Jutterström, S., Landa, C. S., Lauvset, S. K., Michaelis, P., Murata, A., Pérez, F. F., Pfeil, B., Schirnack, C., Steinfeldt, R., Suzuki, T., Tilbrook, B., Velo, A., Wanninkhof, R., and Woosley, R. J.: An updated version of the global interior ocean biogeochemical data product, GLODAPv2.2020, *Earth Syst. Sci. Data*, 12, 3653–3678, <https://doi.org/10.5194/essd-12-3653-2020>, 2020.

Pastor, F., and Khodayar, S.: Marine heat waves: Characterizing a major climate impact in the Mediterranean, *EGU General Assembly 2023*, Vienna, Austria, 24–28 Apr 2023, EGU23-13058, <https://doi.org/10.5194/egusphere-egu23-13058>, 2023.

REALE, M., COSSARINI, G., LAZZARI, P., Lovato, T., Bolzon, G., Masina, S., Solidoro, C., and Salon, S.: Acidification, deoxygenation, and nutrient and biomass declines in a warming Mediterranean Sea, *Biogeosciences*, 19, 4035–4065, <https://doi.org/10.5194/bg-19-4035-2022>, 2022.

Ribotti, A., Sorgente, R., Pessini, F., Cuceo, A., Quattrocchi, G., and Borghini, M.: Twenty-one years of hydrological data acquisition in the Mediterranean Sea: quality, availability, and research, *Earth Syst. Sci. Data*, 14, 4187–4199, <https://doi.org/10.5194/essd-14-4187-2022>, 2022.

Field Code Changed

Field Code Changed

Field Code Changed

Field Code Changed

Field Code Changed

Field Code Changed

Field Code Changed

Field Code Changed

Field Code Changed

Field Code Changed

Field Code Changed

1446 Schroeder, K., Tanhua, T., Bryden, H., Alvarez, M., Chiggiato, J., and Aracri, S.: Mediterranean Sea Ship-based
1447 Hydrographic Investigations Program (Med SHIP), Oceanography, 28, 12–15,
1448 <https://doi.org/10.5670/oceanog.2015.71>, 2015.
1449 Schroeder, K., Kovačević, V., Civitarese, G., Velaoras, D., Álvarez, M., Tanhua, T., Jullio, L., Coppola, L., Bensi,
1450 M., Ursella, L., Santinelli, C., Giani, M., Chiggiato, J., Aly-Eldeen, M., Assimakopoulou, G., Bachi, G., Bogner,
1451 B., Borghini, M., Cardin, V., Cornec, M., Giannakourou, A., Giannoudi, L., Gogou, A., Golbol, M., Or Hazan, O.,
1452 Karthäuser, C., Kralj, M., Krasakopoulou, E., Matić, F., Mihanović, H., Muslim, S., Papadopoulos, V.P., Parinos,
1453 C., Paulitschke, A., Pavlidou, A., Pitta, E., Protopapa, M., Rahav, E., Raveh, O., Renieris, P., Reyes-Suarez, N.,
1454 C., Rousselaki, E., Silverman, J., Souvermezoglou, E., Urbini, L., Zer, C., and Zervoudaki, S.: Seawater physics
1455 and chemistry along the Med SHIP transects in the Mediterranean Sea in 2016, Sci. Data, 11, 52,
1456 <https://doi.org/10.1038/s41597-023-02835-3>, 2024.
1457 Schroeder, K.: TAIPro2022 CRUISE REPORT R/V BELGICA Cruise n. 2022/12 (Version 1), Zenodo,
1458 <https://doi.org/10.5281/zenodo.6918731>, 2022.
1459 Tanhua, T., Brown, P. J., and Key, R. M.: CARINA: nutrient data in the Atlantic Ocean, Earth Syst. Sci. Data, 1,
1460 7–24, <https://doi.org/10.5194/essd-1-7-2009>, 2009.
1461 Tanhua, T.: Matlab Toolbox to Perform Secondary Quality Control (2nd QC) on Hydrographic Data, ORNL
1462 CDIAC 158, Carbon Dioxide Inf. Anal. Center, Oak Ridge Natl. Lab., U.S. Dep. Energy, Oak Ridge, Tennessee,
1463 158, <https://doi.org/10.1002/lom3.10050>, 2010.
1464 Tanhua, T.: Hydrochemistry of water samples during MedSHIP cruise Talpro, PANGAEA,
1465 <https://doi.org/10.1594/PANGAEA.902293>, 2019a.
1466 Tanhua, T.: Physical oceanography during MedSHIP cruise Talpro [dataset], PANGAEA,
1467 <https://doi.org/10.1594/PANGAEA.902330>, 2019b.
1468 Uchida, H., Johnson, G. C. and McTaggart, G. C.: CTD Oxygen Sensor Calibration Procedures. In, The GO-SHIP
1469 Repeat Hydrography Manual: A Collection of Expert Reports and Guidelines. Version 1, (eds Hood, E.M., C.L.
1470 Sabine, and B.M. Sloyan), 17pp. (IOCCP Report Number 14; ICPO Publication Series Number 134),
1471 <https://doi.org/10.25607/OBP-1344>, 2010.

Field Code Changed

Field Code Changed

Field Code Changed

Field Code Changed

Field Code Changed

Field Code Changed

Field Code Changed

Field Code Changed